A Systematic Approach for Performance Comparisons of NO_x Converter Designs

by

Michelle Bendrich

A thesis submitted in partial fulfillment of the requirements for the degree of

Master of Science

in

Chemical Engineering

University of Alberta

Department of Chemical & Materials Engineering

Abstract

In today's vehicle applications, Selective Catalytic Reduction (SCR) ammonia dosing is completed using complex control algorithms that need to be parameterized for the individual catalytic converter technology. The parameterization of these control strategies is not always completed during the early design phase (i.e., simulation studies and laboratory tests), as this procedure is very time consuming. This results in catalytic converter screenings being completed with dosing strategies that do not allow for the observation of the true potential of each catalytic converter. Therefore, a challenge arises in the effective design of catalytic converters.

This work presents a simulation-based method for the automated optimization of a simple ammonia dosing strategy, which can easily be used for simulations during the early catalytic converter design phase. The dosing strategy relies on a look-up table whose entries relate a desired ammonia surface coverage to a catalyst temperature. These entries are optimized for a given driving cycle to maximize the NO_x conversion and fulfill the desired ammonia slip constraints. Using this strategy, comparisons of SCR catalyst technologies (iron and copper zeolite SCR) and catalyst volumes during driving cycles are completed. Likewise, the dosing strategy is applied to a catalytic converter configuration consisting of a front-end SCR and a back-end Ammonia Slip Catalyst (ASC) to study how an ASC can assist in meeting regulatory requirements during driving cycles.

To my family, for their constant love & support.

"Go into the world and do well.

But more importantly, go into the world and do good."

- Minor Myers

Acknowledgements

It is amazing to reflect upon my Masters experience and think about the journey over the past two years that brought me to where I am today. I am extremely grateful for the new and old friendships and connections that have helped me to develop more academically and as an individual.

Specifically, I would like to thank my university supervisors, Dr. J. F. Forbes and Dr. R. E. Hayes, for their support and patience throughout my Masters degree. Likewise, this work would have also not been possible without the support of Umicore AG & Co. KG, in particular, Dr. M. Votsmeier, Bastian Opitz and my wonderful colleagues. Every day was a positive learning experience with them, whether it was related to the content in this thesis, the communication of technical information, improving my German, or realizing the importance of having fun while working!

Finally, I am blessed to have two families to thank. The Wolf family for their incredible generosity and many unforgettable memories. To my own family, for always being there for me, for believing in me, and for teaching me to always look at the sunny side of life and to never give up.

Table of Contents

List of Tables

List of Figures

Nomenclature

Symbols

$c_{gas,i}$	concentration of species *i* in the gas phase (mol/m^3)
c_i	concentration of species *i* (mol/m^3)
$c_{p,gas}$	specific heat capacity of the gas phase (J/kg·K)
$c_{p,s}$	specific heat capacity of the solid phase (J/kg·K)
$c_{wc,i}$	concentration of species *i* in the washcoat (mol/m^3)
D_{eff}	effective diffusivity in a catalyst (m^2/s)
D_H	hydraulic diameter (m)
Di	diffusion coefficient of species *i* in nitrogen (m^2/s)
e	deviation from setpoint (unitless)
E_A	activation energy (J/mol)
$\Delta_r H_j$	heat of reaction for reaction *j* (J/mol)
$J_{wc,i}$	diffusive mole flux of component *i* (mol/m^2·s)
k	thermal conductivity (W/m·K)
k_0	reaction rate constant (various units)
$\dot{m}$	mass flow rate (kg/s)
Nu	Nusselt number (unitless)
r_j	reaction rate of reaction j (mol/m^3·s)
R	universal gas constant (8.315 J/mol·K)
Re	Reynolds number (unitless)
Sc	Schmidt number (unitless)

Sh	Sherwood number (unitless)
t	time (s)
T	temperature (K)
T_{cat}	average catalyst temperature (K)
T_{gas}	temperature of the gas phase (K)
T_s	temperature of substrate (K)
T_{wc}	temperature of the gas phase of the washcoat (K)
v_{gas}	average gas velocity (m/s)
$v_{i,j}$	stoichiometric coefficient of species *i* in reaction *j* (unitless)
V	catalytic converter volume (m^3)
x	radial coordinate in cylindrical coordinate system (m)
x_i	mole fraction of species *i* (unitless)
z	axial coordinate in cylindrical coordinate system (m)
z*	dimensionless axial distance (unitless)

Greek Letters

α	heat transfer coefficient ($W/m^2 \cdot K$)
β	reaction order of O_2 in the standard SCR reaction (unitless)
β_i	mass transfer coefficient of species *i* (m/s)
ε	reaction order of O_2 in the ammonia oxidation reaction (unitless)
γ	parameter for surface coverage dependency of ammonia desorption
σ	number of active sites per reactor volume ($1/m^3$)
Θ	surface coverage of ammonia (unitless)

ρ_{gas} density of the gas phase (kg/m^3)

ρ_s density of the solid phase (kg/m^3)

Abbreviations

AOC Ammonia Oxidation Catalyst

ASC Ammonia Slip Catalyst

CDPF Catalyzed Diesel Particulate Filter

DOC Diesel Oxidation Catalyst

ETC European Transient Cycle

FTP Federal Test Procedure

LNT Lean NO_x Trap

SCR Selective Catalytic Reduction

WHTC World Harmonized Driving Cycle

Chapter 1 - Introduction

Meeting the stringent, government imposed emission level regulations is a major challenge for automobile manufacturers. In addition to the reduction of standard pollutants such as CO, hydrocarbons, and NO_x, regulations have recently placed a more significant emphasis on the reduction of CO_2 emissions due to its global warming potential. To lower these CO_2 emissions from automobiles, diesel-powered vehicles are expected to become more dominant, particularly in areas where gasoline-powered vehicles are currently leading (i.e., United States and Canada), owing to their CO_2-reduction potential that results from their higher fuel economy [1, 2]. Despite these advantages compared to gasoline vehicles, diesel vehicles typically emit more particulate matter (PM) and oxides of nitrogen (NO_x).

To ensure that lower CO_2 emission rates are achieved, the new Euro 6 emission regulations have adopted a colder driving cycle, which is used for vehicle certification and has been designed to represent actual automotive behavior [3]. In terms of diesel vehicle emissions, the lower temperatures make it more challenging to meet the NO_x limits owning to urea-injection difficulties, which is explained shortly, and catalyst effectiveness at lower temperatures [1, 2]. This challenge calls upon improved NO_x removal, or deNOx, after-treatment systems. The discussion of Real Driving Emissions (randomly arranged short vehicle behavior segments) in future European regulations will also make emission control more difficult, yet ensure that the after-treatment systems are more robust [4].

Two major technologies currently exist for NO_x removal in diesel-powered vehicles: lean NO_x traps (LNT) and selective catalytic reduction (SCR) [5]. LNTs typically use a precious metal such as platinum as the catalyst and an adsorber such as barium supported on Al_2O_3. The LNT adsorbs and stores the NO_x under fuel-lean conditions; however, the amount of NO_x stored will reach saturation limits, resulting in NO_x slipping from the system. The adsorbed NO_x is reduced by CO and hydrocarbons during fuel-rich conditions. Ammonia can also be formed during these rich conditions and therefore, recent focus has been on combining the LNT with a succeeding SCR, whose process is discussed next [2]. Some of the LNT's challenges, which must be overcome, include the fuel-penalty during rich conditions and control under transient engine operation [6]. Additionally, the precious metal used in LNTs increase the overall system cost; however, this amount has been reduced through system developments and improvements [2].

Selective catalytic reduction was the method of choice in Europe to meet the Euro 4 and Euro 5 regulations. Vanadium-based catalysts were initially used for SCR, due to their good selectivity for N_2 at lower temperatures; however, the catalyst showed deactivation at higher temperatures. Therefore, for many applications, copper and iron ion-exchanged zeolite catalysts have become the catalyst of choice for SCR due to their excellent activity and nitrogen selectivity [7].

SCR only requires lean-gas conditions and operates on the principle that a reducing agent, ammonia, is added to the exhaust system to convert the NO_x to nitrogen. The ammonia is generated on-board the vehicle through the hydrolysis of urea, provided

the inlet gas temperature is high enough to allow for the hydrolysis reaction to occur. The SCR catalyst is able to adsorb and desorb the ammonia, which is beneficial if too much or too little has been added to the system; however, a sharp increase in load and engine speed, for example due to acceleration, can cause an increase in catalyst temperature, resulting in a decrease in the storage capacity of ammonia [8]. This can result in a significant amount of ammonia slip and presents the major challenge of designing an ammonia dosing strategy that maximizes the NO_x conversion while limiting the ammonia slip. One potential method of improving the performance of the deNOx converter system is the addition of an Ammonia Slip Catalyst (ASC) as a short-zone after the SCR to eliminate the excess ammonia leaving the SCR-brick [9].

Numerical simulation has been shown to be beneficial in reducing the time and cost in the design and development of after-treatment systems [10]. It has allowed one to gain an understanding of a system for the assessment of reactor configurations (e.g. geometrical properties) and the development of operating strategies before test bench runs.

In terms of the SCR converter, a variety of complex control algorithms have been developed for the ammonia dosing control problem; however, they need to be parameterized for each catalyst technology [11]. While this procedure is time consuming, the parameterization process of these control strategies is usually only conducted once a decision for a catalyst and system layout has been made. Consequently, simulations and experimental tests are either carried out with oversimplified dosing strategies (e.g. constant NH_3/NO_x ratio) or existing strategies

optimized for a different catalytic converter during the early converter design phase. This results in screenings being completed with dosing strategies that do not allow for the observation of the true potential of each catalytic converter [12].

Therefore, a challenge arises in the effective design of catalytic converters. An ammonia dosing strategy needs to be developed that can easily be parameterized and applied to different converter configurations to evaluate their performance. Such a strategy would allow for the converter design and operation strategy to be completed simultaneously, which would assist with the preliminary design phase (i.e., simulation studies and laboratory tests) and ensure that meaningful comparisons and appropriate decisions are made.

1.1 Thesis Objective

This thesis presents a method for the automated optimization of an ammonia dosing strategy for the SCR that can be used in the preliminary catalytic converter design phase (i.e., simulation studies, laboratory tests). This strategy should maximize the NO_x conversion over a transient driving cycle, while maintaining the ammonia slip below a set limit.

Using the proposed ammonia dosing strategy, the comparisons of SCR catalyst technologies (iron and copper zeolite SCR) and catalyst volumes during driving cycles can be completed. The importance of completing converter system design and the parameterization of the operating strategy simultaneously is demonstrated through screening comparisons with catalytic converters using pre-existing and over-simplified (constant NH_3/NO_x ratio) dosing strategies.

The dosing strategy is also used on a combined front-end SCR and back-end ASC to study how an ASC can assist in meeting regulatory requirements during driving cycles. An investigation of whether it allows for ammonia to be added to the system more aggressively and, as a result, increase the NO_x conversion is described.

1.2 References

[1] I. Nova, E. Tronconi, Urea-SCR Technology for deNOx After Treatment of Diesel Exhausts (2014).

[2] T.J. Wallington, C.K. Lambert, W.C. Ruona, Diesel vehicles and sustainable mobility in the U.S., Energy Policy 54 (2013) 47-53.

[3] S. Samuel, L. Austin, D. Morrey, Automotive test drive cycles for emission measurement and real-world emission levels - a review, Proceedings of the Institution of Mechanical Engineers, Part D: Journal of Automobile Engineering 216 (2002) 555-564.

[4] M. Weiss, P. Bonnel, R. Hummel, N. Steininger, A complementary emissions test for light-duty vehicles: Assessing the technical feasibility of candidate procedures EUR 25572 EN (2013).

[5] T.V. Johnson, Review of Selective Catalytic Reduction (SCR) and Related Technologies for Mobile Applications, in: I. Nova, E. Tronconi (Eds.), , Springer New York, 2014, pp. 3-31.

[6] W.S. Epling, L.E. Campbell, A. Yezerets, N.W. Currier, J.E. Parks, Overview of the Fundamental Reactions and Degradation Mechanisms of NOx Storage/Reduction Catalysts, - Catalysis Reviews (2007) - 163.

[7] M.P. Harold, P. Metkar, M.P. Harold, Lean NOx Reduction by NH3 on Fe-Exchanged Zeolite and Layered Fe/Cu Zeolite Catalysts: Mechanisms, Kinetics, and

Transport Effects, in: I. Nova, E. Tronconi (Eds.), , Springer New York, 2014, pp. 311-356.

[8] M. Koebel, M. Elsener, M. Kleemann, Urea-SCR: a promising technique to reduce NOx emissions from automotive diesel engines, Catalysis Today 59 (2000) 335-345.

[9] A. Scheuer, W. Hauptmann, A. Drochner, J. Gieshoff, H. Vogel, M. Votsmeier, Dual layer automotive ammonia oxidation catalysts: Experiments and computer simulation, Applied Catalysis B: Environmental 111–112 (2012) 445-455.

[10] A. Güthenke, D. Chatterjee, M. Weibel, B. Krutzsch, P. Kočí, M. Marek, I. Nova, E. Tronconi, Current status of modeling lean exhaust gas aftertreatment catalysts, in: Guy B. Marin (Ed.), Advances in Chemical Engineering, Academic Press, 2007, pp. 103-283.

[11] A. Schuler, M. Votsmeier, P. Kiwic, J. Gieshoff, W. Hautpmann, A. Drochner, H. Vogel, NH3-SCR on Fe zeolite catalysts – From model setup to NH3 dosing, Chem. Eng. J. 154 (2009) 333-340.

[12] W. Hauptmann, M. Votsmeier, H. Vogel, D.G. Vlachos, Modeling the simultaneous oxidation of CO and H2 on Pt - Promoting effect of H2 on the CO-light-off, Appl. Catal., A 397 (2011) 174-182.

Chapter 2 - Simulation Study of SCR Catalysts with Individually Adjusted Ammonia Dosing Strategies: A Practical Optimization Approach

A version of this chapter was submitted to the Chemical Engineering Journal in September 2014 as: B. Opitz, M. Bendrich, A. Drochner, H. Vogel, R. E. Hayes, J. F. Forbes, M. Votsmeier, Simulation Study of SCR Catalysts with Individually Adjusted Ammonia Dosing Strategies.

Stringent, government imposed, emission standards have resulted in continuous advances in the automobile industry to develop techniques to reduce emissions during the more demanding driving test cycles. In the case of reducing NO_x emissions in diesel vehicles, selective catalytic reduction (SCR) has been investigated over the years and is a successful method currently used to reduce NO_x emissions [1, 2].

In the SCR process, ammonia, the reducing agent, is generated onboard through the hydrolysis of urea, provided the inlet gas temperature is high enough to allow for the hydrolysis reaction to occur [3]. The ammonia can then react with the NO_x gas via one of the following key SCR reactions:

Standard SCR: $4NH_3 + 4NO + O_2 \rightarrow 4N_2 + 6H_2O$ (R1)

Fast SCR: $4NH_3 + 2NO + 2NO_2 \rightarrow 4N_2 + 6H_2O$ (R2)

NO_2 SCR: $8NH_3 + 6NO_2 \rightarrow 7N_2 + 12H_2O$ (R3)

Reaction (R1) is dominant when there is more NO than NO_2 in the feed whereas Reaction (R3) is more dominant when the opposite is true. Reaction (R2) is the fastest of the SCR reactions and prevails when the amount of NO to NO_2 is 1:1.

The SCR catalysts are also able to adsorb or desorb the ammonia, which is beneficial when too much has been dosed or more is needed [4]; however, the storage capacity of ammonia in the catalyst decreases strongly with an increase in temperature [1]. Therefore, a sharp increase in load can result in a significant amount of ammonia slip. This means that the amount of ammonia added to the system needs to be controlled and presents the need for an optimized urea dosing strategy, where NO_x conversion is maximized, while maintaining the ammonia slip below a currently non-regulated acceptable level.

In today's vehicle applications, ammonia dosing is completed using complex control algorithms that need to be parameterized for the individual catalyst technology [5]. Feed-forward control strategies based on the SCR catalyst surface reactions with some compensation for ammonia storage are commonly used for open-loop control [6]. For instance, a Nominal Stoichiometric Ratio (NSR) map with a limiter for ammonia slip peaks has been investigated as an open-loop or feed-forward control strategy [7]. A feed-forward controller accounting for the steady state ammonia usage and storage level compensation using observers, was also examined [5]. Closed-loop feedback strategies with either an ammonia sensor [8] or NO_x emissions feedback

have been developed [7]. In this context, numerical simulation has become an important tool for the development of control strategies [9].

The parameterization of these control strategies is not always completed during the early design phase, consisting of simulation studies and laboratory tests, as this procedure can be time consuming. This results in using either oversimplified dosing strategies (e.g., constant NH_3/NO_x ratio) or specific strategies for different catalysts.

This work presents a practical simulation-based method for the automated optimization of an ammonia dosing strategy, which can easily be used for simulations and laboratory tests during catalyst development. This method consists of a feedback control system, whose setpoint is determined via a look-up table that relates the optimal average surface coverage of ammonia to the average catalyst temperature. The entries of the look-up table are optimized over a driving cycle such that the NO_x conversion is maximized under ammonia slip restrictions. A variety of other constraints are also considered, such as urea dosing constraints to account for the temperature-sensitivity of the hydrolysis process and equipment limitations.

Simulation-based screenings and comparisons of catalytic converter designs were completed using individually optimized ammonia dosing profiles. The use of simulation-based catalytic converter screenings demonstrated that the true potential of a design can only be determined under its own individually adjusted conditions.

2.1 Ammonia Dosing Control Strategy

The presented ammonia dosing strategy is a simulation-based feedback control system, based on control strategies traditionally used in vehicle SCR applications [5, 7]. It is important to note that this dosing strategy is meant for simulations and laboratory tests, and is not intended to replace complex control algorithms used in vehicle applications. It is intended solely to determine an optimal dosing strategy in the rapid development and design of catalysts.

The block-diagram of the controlled system is illustrated in Figure 1. In this set-up, the amount of ammonia added to the SCR catalyst at any time is dictated by an optimized look-up table, which relates average catalyst temperatures to optimal average ammonia surface coverages. The usage of this table and functionality of the proposed dosing strategy is described in more detail via the following algorithm:

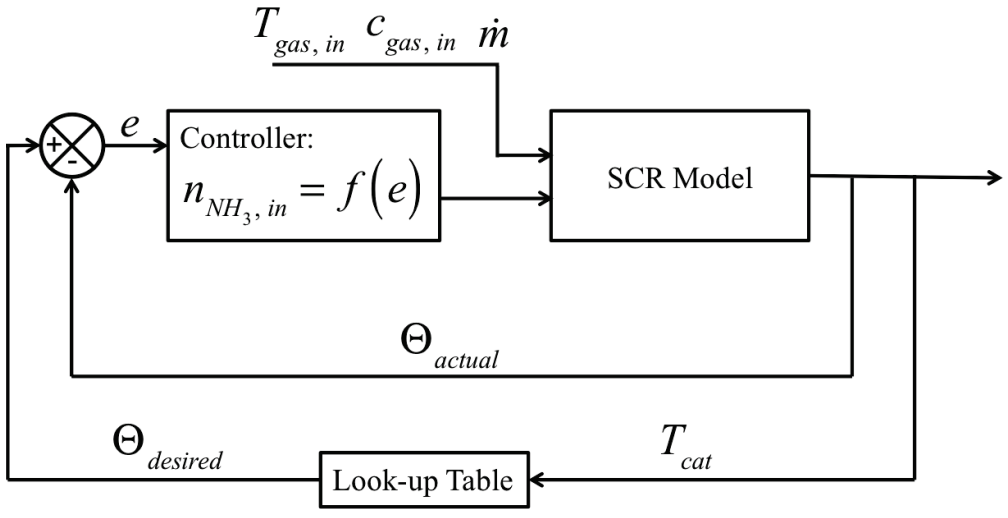

Figure 1. Block-diagram of the model-based feedback loop utilizing the optimized look-up table.

1) Starting at a given time (t), ammonia ($n_{NH3,in}(t)$) is injected into the exhaust gas stream in front of the catalyst. At this time, the SCR model (described in Section 2.2.1 and 2.2.2) is used to calculate the output variables including the average catalyst temperature ($T_{cat.}(t)$) and actual average ammonia surface coverage ($\Theta_{act.}(t)$).
2) The look-up table is then used to determine the setpoint, or desired average ammonia surface coverage ($\Theta_{des.}(t)$), for the current catalyst temperature via linear interpolation between table entries. Knowing the actual average ammonia surface coverage ($\Theta_{act.}(t)$), the deviation from the setpoint ($e(t)$) can be determined.
3) The amount of ammonia to be added to the system at the next time instant can then be calculated as:

$$n_{\mathrm{NH_3in}(t+\Delta t)} = \begin{cases} [\Theta_{des.}(t) - \Theta_{act.}(t)] \cdot \sigma \cdot V, & \text{if } \Theta_{des.}(t) > \Theta_{act.}(t) \\ 0, & \text{otherwise} \end{cases} \quad (1)$$

where $\Theta(t)$ represents the average ammonia surface coverage, σ the number of active sites per reactor volume and V the catalyst volume. This feedback control procedure, consisting of the three steps listed above, can then be completed successively for each time instant of a given driving cycle.

To achieve a desired objective, and therefore have a suitable controller, the values of the look-up table must be optimized for a given case over a driving cycle. In this work, the table entries were optimized to ensure NO_x conversion was maximized over a driving cycle, under a variety of constraints (e.g., maximum allowed ammonia slip).

Experimentally obtained input data from an engine test bench for different driving cycles (e.g. WHTC, FTP, and ETC) were used.

An optimization algorithm was used to search the space of look-up table entry values to meet the desired objective, and is further discussed in the Methods section.

2.2 Methods

The reactor model used to simulate the SCR is described in Sections 2.2.1 and 2.2.2. This model was developed and provided by Umicore AG & CO. KG in the form of a black-box and is briefly described for completeness.

2.2.1 1-D Single Channel Model

The reactor model used in this work is based on the geometry of a honeycomb monolith that consists of numerous parallel open channels. As the geometrical properties of all channels, their catalyst distribution, and the inlet conditions are assumed identical, the flow through the monolith is modelled by solving the corresponding mass and energy balances for a one-dimensional single open channel. One-dimensionality is assumed such that the gas phase temperature T_{gas} and concentration $c_{gas,i}$ of the gas species *i* are mixing cup values. The transport from the gas phase to the surface is described by heat and mass transfer coefficients. Therefore, the concentration profiles in the gas phase $c_{gas,i}$ and gas phase in the washcoat $c_{wc,i}$ are computed according to the following plug flow model:

$$\frac{\partial c_{gas,i}}{\partial t} = -v_{gas} \cdot \frac{\partial c_{gas,i}}{\partial z} - \beta_i \cdot \frac{4}{D_H} \left(c_{gas,i} - c_{wc,i} \right) \tag{2}$$

$$\frac{dc_{wc,i}}{dt} = \Phi \cdot \beta_i \cdot (c_{gas,i} - c_{wc,i}) + \sum_j (v_{i,j} \cdot r_j) \tag{3}$$

where the inlet condition for equation (2) is $c_{gas,i}(t) = c_{gas,i\_in}(t)$ at $z = 0$. The initial condition for equation (3) is $c_{wc,i}(z, t = 0\ s) = c_{gas,i\_in}(t = 0\ s)/100$. In equations (2) and (3) the variable z is the axial position in the channel, v_{gas} is the average gas velocity, D_H is the hydraulic diameter and $c_{wc,i}$ is the concentration of species i at the washcoat surface. The geometrical factor Φ is the specific surface area between gas and solid phase per washcoat volume. The position dependent mass transfer coefficient $\beta_{i,}$ is computed via the Sherwood number:

$$Sh = \frac{\beta_i \cdot D_H}{D_i} \tag{4}$$

where D_i is the diffusion coefficient of species i in nitrogen, calculated using the semi-empirical method from Fuller et al. [10]. Taking into account the effect of developing concentration profiles and laminar flow, the position dependent Sherwood Number Sh is computed via equation (5) using the asymptotic Sherwood Number for a constant wall concentration (Sh_∞) and circular cross section [11].

$$Sh = 3.657 + 8.827\,(1000 \cdot z^*)^{-0.545} \exp(-48.2 \cdot z^*) \tag{5}$$

In equation (5), z* represents a dimensionless axial distance which is calculated through equation (6), where Re is the Reynolds number and Sc is the Schmidt number [11].

$$z^* = \frac{(z/D_H)}{(Re \cdot Sc)} \tag{6}$$

The gas phase temperature T_{gas} and the substrate temperature T_s are computed by solving the following energy balances:

$$\frac{\partial T_{gas}}{\partial t} = -v_{gas} \cdot \frac{\partial T_{gas}}{\partial z} - \alpha \cdot \frac{4}{D_H \cdot \rho_{gas} \cdot c_{p,gas}} \cdot (T_{gas} - T_s) \tag{7}$$

$$\frac{dT_s}{dt} = \Phi \cdot \frac{\alpha}{\rho_s \cdot c_{p,s}} \cdot (T_{gas} - T_s) + \frac{\sum_j (\Delta_r H_j \cdot r_j)}{\rho_s \cdot c_{p,s}} \tag{8}$$

where the inlet condition for equation (7) is $T_{gas}(t) = T_{gas\_in}(t)$ at $z = 0$. The initial condition for equation (8) is $T_{s,i}(z, t = 0\ s) = T_{gas\_in}(t = 0\ s)$. In equation (8) the variable r_j is the reaction rate and $\Delta_r H_j$ is the reaction enthalpy of the associated surface reaction j. The heat transfer coefficient, α, is calculated in analogy to the mass transfer coefficient (β_i) via the Nusselt number in equation (9). The Nusselt number is also calculated via the correlation of equation (5); however, z* in equations (5) and (6) is replaced by the reciprocal Graetz number Gz^{-1} and the Schmidt number Sc in equation (6) is substituted with the Prandtl number (Pr).

$$Nu = \frac{\alpha \cdot D_H}{k} \tag{9}$$

To solve the system of equations, the pseudo-steady state assumption is made such that the gas phase concentrations are assumed to be at steady state. Therefore, only equations (3) and (8) are treated in a transient manner and the resulting system of equations are numerically integrated using the DASSL solver. A detailed description of the monolith reactor model can be found in [12].

2.2.2 Kinetic Model for the SCR Washcoat

The SCR catalyst kinetics have been studied extensively in the literature and several kinetic models have been published [5, 13-16]. The kinetic model used in this work was previously published in [5] and [13]. The model used takes into account the reactions involving NH_3, NO and NO_2 occurring under typical exhaust conditions and the reaction scheme is presented in Table 1.

Table 1. Reactions and rate equations for the SCR washcoat kinetic model.

Reaction	**Rate Equation**
NH_3 adsorption/desorption: $NH_3 + [*] \leftrightarrow NH_3*$	$r_{\text{ads},NH_3} = k_{0,\text{ads}} \cdot c_{NH_3} \cdot (1-\Theta)$ $r_{\text{des},NH_3} = k_{0,\text{des}} \cdot \exp\left(\frac{-E_{A,\text{des}}}{R \cdot T} \cdot (1-\gamma \cdot \Theta)\right) \cdot \Theta$
Standard SCR: $4NH_3* + 4NO + O_2 \rightarrow 4N_2 + 6H_2O + 4[*]$	$r_{NO} = k_{0,NO} \cdot \exp\left(\frac{-E_{A,NO}}{R \cdot T}\right) \cdot \frac{c_{NO} \cdot \Theta}{1 + K_{NH_3} \cdot \Theta/(1-\Theta)} \cdot \left(\frac{x_{O_2}}{0.06}\right)^{\beta}$
Fast SCR: $2NH_3* + NO + NO_2 \rightarrow 2N_2 + 3H_2O + 2[*]$	$r_{\text{fastSCR}} = k_{0,\text{fastSCR}} \cdot \exp\left(\frac{-E_{A,\text{fastSCR}}}{R \cdot T}\right) \cdot x_{NO} \cdot x_{NO_2} \cdot \Theta$
NO_2 SCR: $8NH_3* + 6NO_2 \rightarrow 7N_2 + 12H_2O + 8[*]$	$r_{NO_2\text{-SCR}} = k_{0,NO_2\text{-SCR}} \cdot \exp\left(\frac{-E_{A,NO_2\text{-SCR}}}{R \cdot T}\right) \cdot x_{NO_2} \cdot \Theta$

Table 1. Reactions and rate equations for the SCR washcoat kinetic model.

Reaction	**Rate Equation**
NH_3 Oxidation: $4NH_3 * + 3O_2 \rightarrow 2N_2 + 6H_2O + 4[*]$ $2NH_3 * + 3NO_2 \rightarrow N_2 + 3NO + 3H_2O + 2[*]$	$r_{\mathrm{NH_3\text{-}Ox,O_2}} = k_{0,\mathrm{NH_3\text{-}Ox,O_2}} \cdot \exp\left(\frac{-E_{A,\mathrm{NH_3\text{-}Ox,O_2}}}{R \cdot T}\right) \cdot \left(\frac{x_{\mathrm{O_2}}}{0.06}\right)^{\varepsilon} \cdot \Theta$ $r_{\mathrm{NH_3\text{-}Ox,NO_2}} = k_{0,\mathrm{NH_3\text{-}Ox,NO_2}} \cdot \exp\left(\frac{-E_{A,\mathrm{NH_3\text{-}Ox,NO_2}}}{R \cdot T}\right) \cdot x_{\mathrm{NO_2}} \cdot \Theta$
NO/NO_2 Equilibrium: $NO + 0.5O_2 \leftrightarrow NO_2$	$r_{\mathrm{NO\text{-}Ox}} = k_{0,\mathrm{NO\text{-}Ox}} \cdot \exp\left(\frac{-E_{A,\mathrm{NO\text{-}Ox}}}{R \cdot T}\right) \cdot \left(x_{\mathrm{NO}} \cdot x_{\mathrm{O_2}}^{0.5} - \frac{x_{\mathrm{NO_2}}}{K_{eq}}\right)$

In addition to the reaction scheme, an empirical correction for the rate of ammonia oxidation in presence of NO/NO_2 was implemented in the kinetic model [17]. This is necessary because Schuler et al. [5] experimentally observed a temperature-varying NH_3/NO stoichiometric ratio greater than one, in the case of the standard SCR reaction. Therefore, temperature dependent stoichiometric factors for the ammonia consumption during standard (R1) and fast SCR (R2) were implemented, leading to an increased rate of ammonia oxidation by O_2 [17].

$$r_{\mathrm{NH_3\text{-}Ox,O_2}} = r^{0}_{\mathrm{NH_3\text{-}Ox,O_2}} + f_{\mathrm{NO}}(T) \cdot r_{\mathrm{NO}} + f_{\mathrm{NO_2\text{-}SCR}}(T) \cdot r_{\mathrm{NO_2\text{-}SCR}} \qquad (10)$$

where $r^{0}_{\mathrm{NH3\text{-}Ox,O2}}$ is the rate of ammonia oxidation in the absence of NO/NO_2 and $f_{\mathrm{NO}}(T)$ and $f_{\mathrm{NO2\text{-}SCR}}(T)$ are temperature dependent look-up tables for the respective reaction.

The kinetic model was parameterized in [5] for an iron and a copper zeolite SCR catalyst using a large set of experimental data. A detailed description of the stationary and transient data used for parameterization can be found in [5].

2.2.3 Description of the Exhaust Emissions System

In this work, the ammonia dosing profile for an SCR system was optimized for a heavy-duty diesel vehicle during typical test cycles. The exhaust emissions system used consisted of a Diesel Oxidation Catalyst (DOC), the Catalyzed Diesel Particle Filter (CDPF), and the SCR catalyst, where the ammonia was injected between the CDPF and the SCR. A schematic of the set-up can be seen in Figure 2.

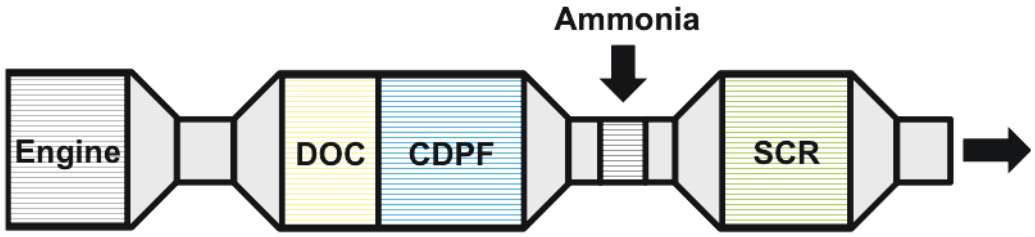

Figure 2. The Exhaust Emission System.

The experimental setup used in Sections 2.3.1 and 2.3.2 consisted of a monolith with a diameter of 10.5", a length of 12", a cell density of 400 cpsi, and a wall thickness of 6.5 mil. The optimization of the ammonia dosing strategy was completed for the World Harmonized Transient Cycle (WHTC).

For the simulation-based comparison of different catalysts (Section 2.3.3 onwards), the experimental setup consisted of a catalyst with a diameter of 12", a length of 8", a cell density of 400 cpsi, and a wall thickness of 6.5 mil. Three different transient driving cycles were used for the optimizations, including the WHTC, the European Transient Cycle (ETC), and the Federal Test Procedure (FTP), where the same engine setup and catalysts were employed to produce consistent input data.

Although the engine speed and load are specified for the driving cycles [19, 20] the input values for the SCR simulation model were the experimental exhaust gas compositions, mass flow rate, and temperature once the gas had passed through the DOC and CDPF. As a result, only the SCR system had to be considered for the optimization process.

2.2.4 Optimization Problem

In this work, the values for six entries in a look-up table were optimized to determine the ammonia dosing strategy, such that the NO_x conversion is maximized over a given driving cycle. A variety of constraints were considered, including the ammonia slip constraints, as the ammonia added at a previous time instant can affect the ammonia slip later in the driving cycle due to transient conditions. The constraints to be satisfied are:

- Maintaining the maximum ammonia slip below a specified level at any time instant. The maximum ammonia slip tends to occur during transient phases, even when no extra ammonia is added to the system. This constraint ensures that surface coverage for the driving cycle is not so high that the slip constraint is exceeded during a temperature increase.
- Maintaining the average ammonia slip below a specified level over the driving cycle. This allows the greater amount of ammonia slip that occurs during the transient conditions to counterbalance the lower amount of ammonia slip during the steady state conditions.
- A maximum amount of ammonia to be added at any time instant. This is to account for the equipment limitations, which can only inject a certain amount of urea-solution into the gas phase entering the SCR system at any given time instant. This value was taken to be 2000 ppm.
- A lower temperature bound at which no urea can be added to the system. As the hydrolysis of urea, thus producing ammonia, only occurs above a certain

temperature, urea may only be added to the system above a specified temperature [21]. Throughout this work the temperature bound was taken to be 180°C.

The last two constraints (equipment limitation and temperature restriction) are implemented into the model such that they always hold true. For example, if the look-up table dictates that an amount greater than 2000 ppm ammonia be added to the system, the maximum of 2000 ppm will be added. Likewise, should the inlet gas temperature fall below 180°C, no ammonia will be added to the system regardless of whether the look-up table dictates otherwise.

Therefore, the resulting optimization problem's objective is to minimize the cumulative NO_x emissions over the given driving cycle, which is represented by equation (11a). The constraints include the model, the average ammonia slip limitation over the driving cycle, and the maximum ammonia slip peak limitation throughout the driving cycle, which are represented by equations (11b) to (11d), respectively. The decision variables are the look-up table's parameters (i.e., entries).

$$\min \sum n_{out,NO_x}(t) \tag{11a}$$

$$\begin{aligned}&\left[x_{out,j}(t+1), x_{wc,j}(t+1), \Theta_j(t+1), T_{out}(t+1), T_s(t+1)\right] \\ &= \mathrm{SCR}_{\mathrm{model}}\left[\dot{m}, x_{in,j}(t), x_{wc,j}(t), \Theta_j(t), T_{in}(t), T_s(t), \text{look-up table}\right]\end{aligned} \tag{11b}$$

$$\bar{x}_{out,NH_3}(t) \leq 10 \text{ ppm} \tag{11c}$$

$$max\left(x_{out,NH_3}(t)\right) \leq 50 \text{ ppm} \tag{11d}$$

In equations (11a) to (11d), the variable $n_{out,NOx}$ represents the moles of NO_x exiting the system, x represents the mole fraction of component j, T the temperature, and $\dot{m}$ the mass flow rate. The subscript wc represents the washcoat phase.

The optimization of the six entry values of the look-up table was completed using a gradient-based algorithm for a constrained, non-linear optimization problem. The degrees of freedom were the six average optimal surface coverage values at six pre-specified temperatures in the look-up table. The starting point was user-defined, the gradients were estimated via finite differences because of the high fidelity SCR simulation model, and the stopping criterion was when the gradient or distance between iterations was below a specified tolerance.

The hardware used for all calculations in this paper was an Intel Core i7-3939K CPU @ 3.20 GHz with 64 GB RAM running CentOS 6.5 as an operating system. A typical optimization took approximately 70 min and 250 function calls.

2.3 Results and Discussion

2.3.1 Optimization Results for Ammonia Dosing Profiles

The entries in the look-up table were first optimized for an iron zeolite SCR catalyst to obtain the maximum NO_x conversion while staying within the maximum ammonia slip constraint of 10 ppm. This was completed for the identical WHTC driving cycle as used by Hauptmann et al. [18], where Figure 3 shows the experimental input temperature profile and input mass flow rate to the SCR catalyst.

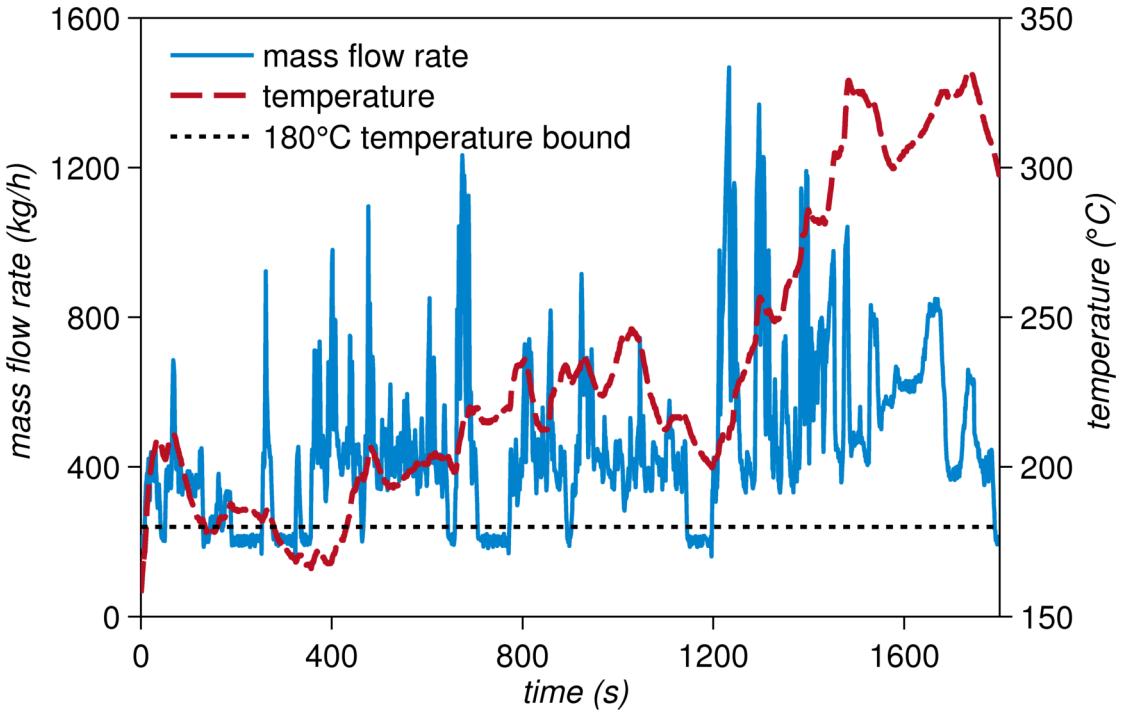

Figure 3. **Gas temperature and mass flow rate input to the SCR system for the WHTC driving cycle, as measured at the engine test bench.**

The optimization was completed according to the method described in Section 4.4, and resulted in the following six parameter look-up table (Table 2).

Table 2. **Optimized look-up table for the iron zeolite SCR catalyst, based on the WHTC driving cycle.**

Temp (K/°C)	400/127	450/177	500/227	550/277	600/327	650/377
Surf. Cov.	0.499	0.341	0.210	0.072	0.039	0.034

The values in the table show that the optimal ammonia surface coverage decreases with an increase in the average catalyst temperature, which is directly linked to the

general trend that the amount of adsorbed ammonia decreases significantly with an increase in temperature. Therefore, the ammonia dosing is much more conservative at higher temperatures to avoid exceeding the acceptable amount of ammonia slip. Figure 4 shows the comparison between the resulting ammonia dosing profile and ammonia slip using the optimized look-up table in Table 2.

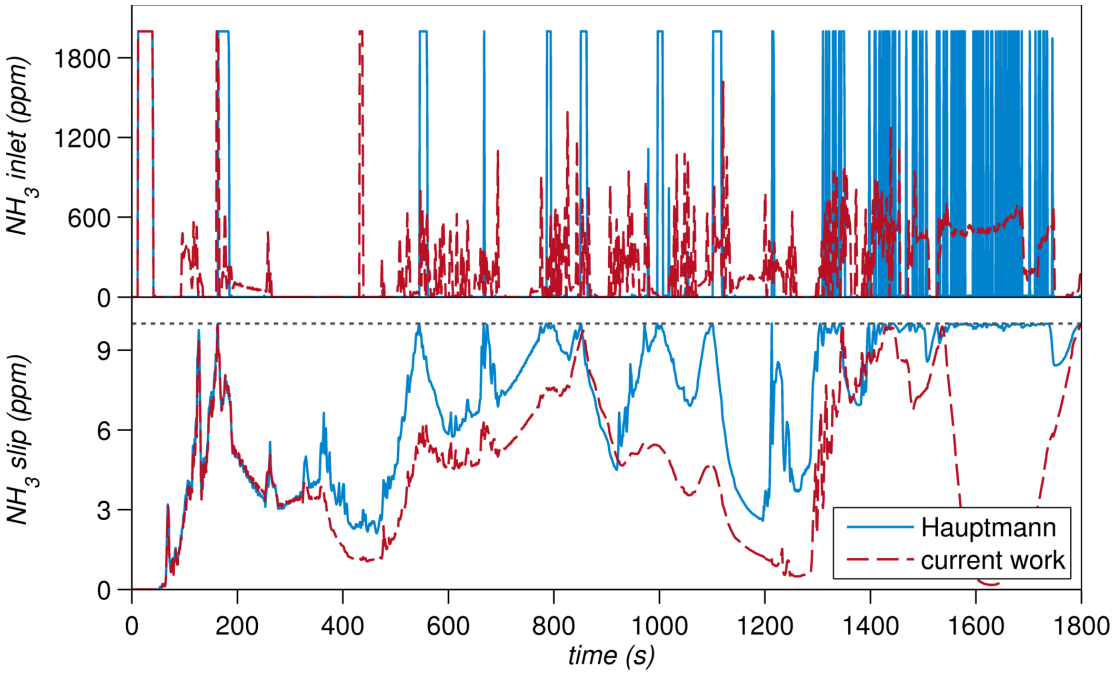

Figure 4. **Optimized ammonia dosing profile for the WHTC driving cycle (top) and the corresponding ammonia slip (bottom).**

Throughout the driving cycle the ammonia concentration at the catalyst outlet did not exceed the 10 ppm maximum criterion, which is shown by the dashed line in Figure 4. Furthermore the look-up table method achieved a total NO_x conversion of 73.2%.

To analyze the proposed dosing strategy further, both the optimal and the actual surface coverage are depicted in Figure 5.

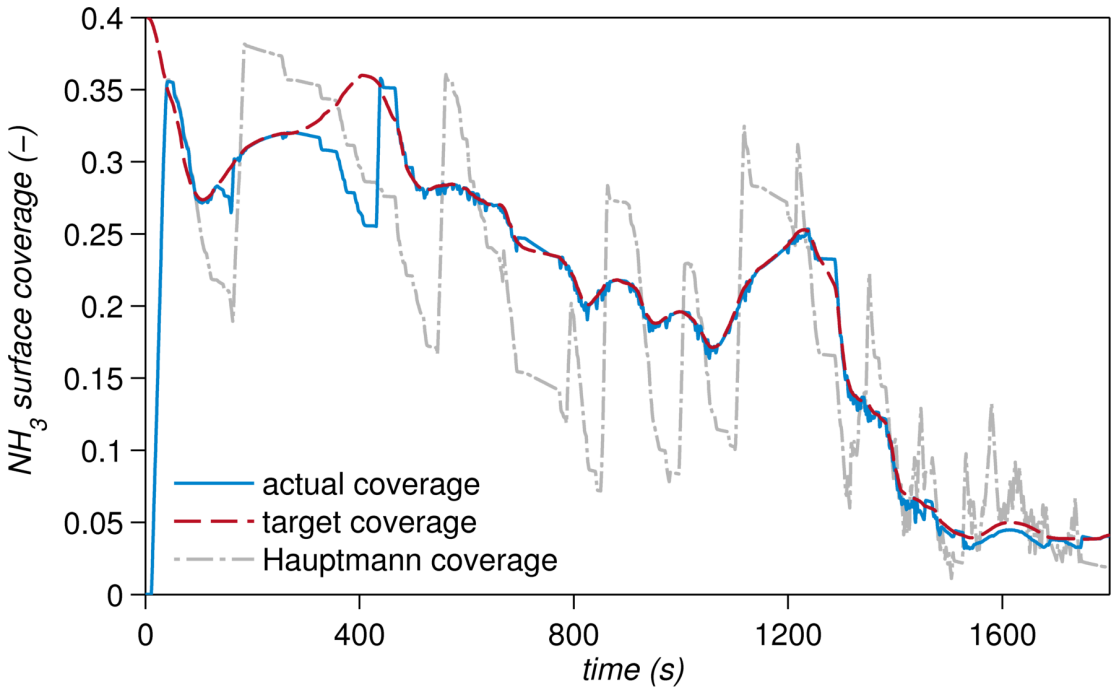

Figure 5. Comparison of the actual and the optimal target ammonia surface coverage for the look-up table method throughout the WHTC driving cycle.

The figure shows that the actual ammonia surface coverage and optimal target coverage agree well throughout the WHTC driving cycle; however, two exceptions arise where the actual coverage is significantly below the optimal value. At the beginning of the cycle, there is no ammonia stored within the washcoat and as the maximum dosing constraint of 2000 ppm is active, it takes several seconds to reach the target coverage value. The second exception occurs at approximately 280 to 430 seconds in the driving cycle. During this period the inlet gas temperature is below the lower bound of 180°C for ammonia dosing, and therefore no ammonia is injected, resulting in a portion of the stored amount being used.

The slight fluctuations in the actual ammonia surface coverage can be linked to the simulation time step, which was set to 1 s. During this time step the concentration of ammonia in the inlet gas flow is held constant, despite minor changes in catalyst temperature and ammonia consumption due to the SCR reaction. Decreasing the simulation time step results in the disappearance of the slight fluctuations, accompanied by a significant increase in total simulation time required for the optimization procedure.

2.3.2 Comparison with Hauptmann et al. [18]

In this section, the look-up table dosing strategy proposed here is compared to the work presented by Hauptmann et al. [18]. The dosing strategy proposed by Hauptmann et al. [18] is an open-loop control strategy that dictates the amount of ammonia to be added at each discrete time step. Using the identical WHTC driving cycle as in Section 5.1 with a 1800 s duration and a 1 s discretization for the simulation model, a 1800 degree of freedom optimization problem is obtained. To reduce the complexity of the optimization problem, Hauptmann et al. [18] presented a simplified heuristic approach based on the assumption that adding the maximum amount of allowed ammonia at each successive time step yields the optimal NO_x conversion over the entire driving cycle. Due to this assumption, the 1800 parameters optimization problem is broken into 1800 sub-optimization problems, which are then sequentially solved. For each sub-optimization problem, Hauptmann et al. [18] computed the maximum ammonia dosage at time t_i, using catalyst conditions at time t_{i-1}, to ensure there was no breakthrough within a given time horizon Δi. This means that for each one-parameter optimization, all future catalyst input conditions

(temperature, mass flow rate, and exhaust gas composition) must be known for the entire time horizon.

Figure 4 compares the ammonia dosing and slip profile using the optimization strategy of Hauptmann et al. [18] and the results obtained using the look-up table strategy. Throughout the driving cycle, neither of the methods exceeded the 10 ppm maximum ammonia slip criterion, which is shown by the dashed line. Hauptmann et al. achieved a total NO_x conversion of 72.1%, while the look-up table method achieved a conversion of 73.2%. This demonstrates that, although the total amount of ammonia added for the two different strategies is similar, the assumption made by Hauptmann et al., which is adding the maximum amount of ammonia allowed at each time instant to ensure an optimal NO_x conversion, is not completely true. In other words, the timing of the dosing plays an important role. This is demonstrated in Figure 5, which shows that the average surface coverage profile for the look-up table method is smoother; whereas the strategy of Hauptmann et al. results in a more uneven profile with higher peaks in the surface coverage. Therefore, the optimization of NO_x conversion using the look-up table method shows that a generally high and constant surface coverage is favorable.

Further shortcomings of Hauptmann's method are the limitations in the choice of constraints. It is only possible to define a maximum slip constraint and not, for example, an average slip constraint or a limitation on the overall amount of ammonia added. The look-up table approach does not suffer this limitation. Another disadvantage is the robustness of the optimized dosing strategy towards other

conditions. Where Hauptmann et al.'s control strategy is open-loop control, its optimized dosing profile is time-dependent and therefore does not take into account any changes in catalyst setup (e.g. dimensions of catalyst) and input conditions (e.g. temperature, mass flow rate, concentration). Therefore the optimized ammonia dosing profile is only valid for the catalyst and driving cycle used for optimization. In the case of the look-up table method, which incorporates feedback, the applicability of the optimized look-up table on other conditions, e.g. different driving cycles or possibly real-driving scenarios, is theoretically possible. This is discussed in more detail in Section 2.3.4.

2.3.3 Importance of Dosing Strategy

This section deals with the application of the ammonia dosing strategy described in Section 2.1. In the following subsections, the optimization of dosing profiles are used for comparison of different catalyst technologies (iron and copper zeolite SCR) and the investigation of the influence of catalyst volume on the SCR performance. Likewise, the importance of an individually adjusted ammonia dosing strategy for each catalyst is demonstrated by comparison with a simple constant alpha dosing strategy.

2.3.3.1 Different Catalyst Materials

For comparison of different catalyst materials, the look-up table optimization was carried out for an iron and a copper zeolite SCR catalyst. As explained in detail in Section 2.2.4, experimental input data for a WHTC driving cycle were used for optimization of the NO_x conversion under the constraint of a maximum of 10 ppm

ammonia slip. Figure 6 shows the performance comparison of the two different SCR technologies. On the left, the performance of the iron and copper zeolite catalyst is compared using a dosing profile optimized for the copper catalyst. The copper catalyst clearly shows a higher NO_x conversion of 87.0% compared to the iron catalyst with 68.7%. On the right, the identical catalysts are compared using a dosing strategy optimized for the iron catalyst. In this case, the iron catalyst shows almost the same NO_x conversion as the copper catalyst, but the copper catalyst does not achieve its full NO_x conversion potential.

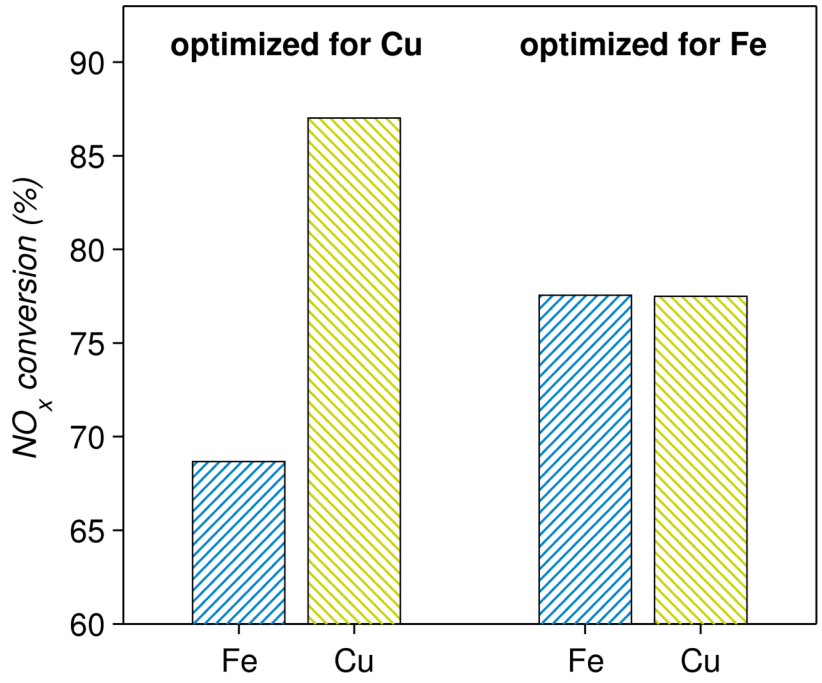

Figure 6. Performance comparison of iron zeolite and copper zeolite catalyst using optimized ammonia dosing profiles for a WHTC driving cycle.

As expected, the performance of the two different catalysts depends upon the ammonia dosing profile used for the analysis. Through the bar graph, it can be seen that both catalysts show a better performance for the WHTC driving cycle with their own respective optimized dosing strategy.

During the catalyst development stages, the dosing strategy used is commonly based on one from a previous catalyst technology. If this approach was used for the iron catalyst dosing strategy in the presented situation, an iron catalyst would have been selected as the next generation of catalysts, despite the significantly higher NO_x conversion using the copper catalyst with its own optimized dosing profile.

2.3.3.2 Different Catalyst Length

Not only is the washcoat technology an important design criterion, but the catalyst volume is as well. To investigate the influence of the catalyst volume, simulations were performed for a 4" and 8" long catalyst with a constant diameter of 12". The optimization of the look-up table entries was carried out for the iron zeolite SCR catalyst using the WHTC driving cycle. Additionally, the optimization was extended to include more realistic constraints for practical vehicle applications. The average slip over the driving cycle was limited to 10 ppm and maximum ammonia peaks of 50 ppm were allowed.

2.3.3.2.1 Comparison with optimized dosing profiles

This section deals with the influence of an adjusted dosing strategy for the comparison of catalysts with different volumes. Therefore, as done with the different catalyst materials, the performance of a 4" and 8" catalyst was compared using the optimized dosing strategy for the two catalyst lengths. The results of this comparison are presented in Figure 7.

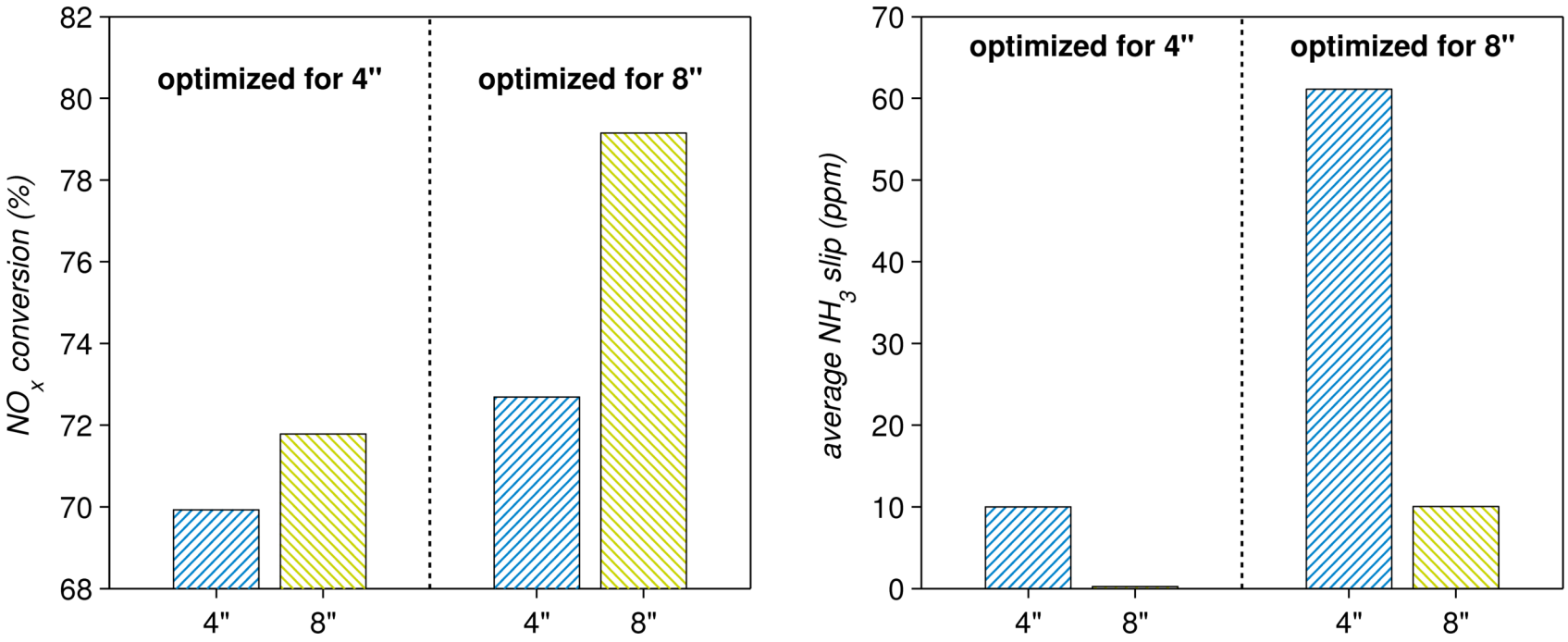

Figure 7. Comparison of the NO_x conversion (left) and the average ammonia slip (right) of an iron zeolite SCR catalyst for two different lengths and dosing strategies.

As expected, the NO_x conversion increases with catalyst length when using the optimized dosing profiles for the 4" and 8" catalyst because of the resulting increased residence time. The increase in NO_x conversion when using the 4" optimized dosing profile for the two catalyst lengths is 1.8%, and 6.4% when using the 8" optimized profile. Both of these increases in NO_x conversion with catalyst length are significantly lower compared to the difference between the respective optimized cases (9.2%). This inferior performance difference can be explained by the two optimized ammonia dosing strategies. The dosing profile optimized for the 4" catalyst adds less ammonia to the system than the profile optimized for the 8" catalyst. Therefore, when using the dosing profile optimized for the 4" catalyst, the 8" catalyst suffers significant under-dosing, which can be seen by its almost non-existent average ammonia slip in Figure 7. When the profile optimized for the 8" catalyst is used for the 4" catalyst, the average ammonia slip is very high, demonstrating significant ammonia over-dosing for this system resulting in an increased NO_x conversion.

In terms of catalyst screening and design, these results reveal that without an individually optimized dosing profile for each catalyst length, the true potential of any catalyst configuration cannot be clearly determined.

2.3.3.2.2 Comparison with dosing at constant alpha value

Simulations or experimental tests are typically completed using oversimplified dosing strategies because the parameterization procedure is time consuming and therefore usually only conducted once a decision for a catalyst and system configuration has been made. Therefore, a constant alpha dosing strategy was completed for a 4" and 8"

SCR catalyst and is compared to the optimized dosing strategies for each of the respective catalysts.

Throughout the constant alpha dosing strategy, the equipment limitation and temperature dosing constraint described in Section 2.2.4 were considered to facilitate comparison of results with the look-up table dosing strategy in Section 2.3.3.2.1. Figure 8 depicts the NO_x conversion achieved along with average ammonia slip for various constant alpha dosing rates.

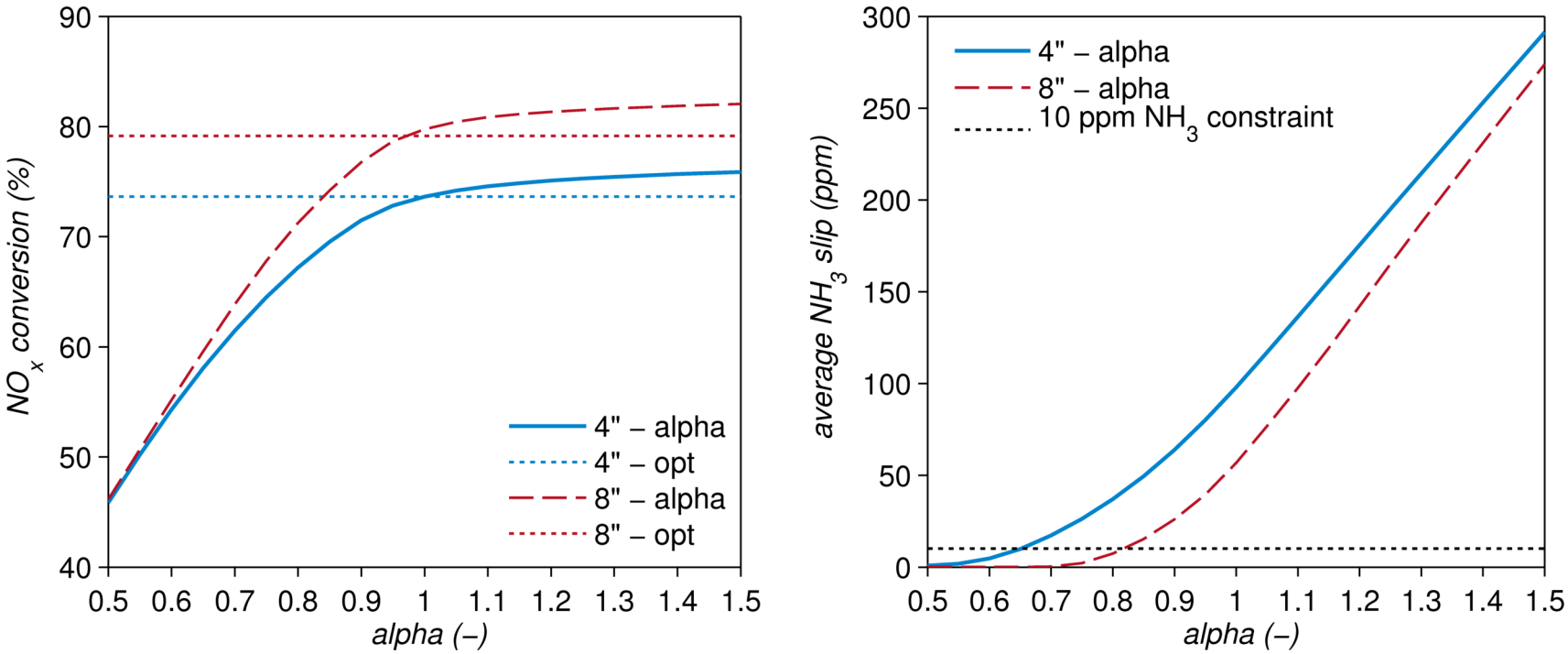

Figure 8. NO_x conversion and average ammonia slip for the 4" and 8" long SCR catalyst using a constant alpha value as the dosing strategy.

As expected, Figure 8 shows that the NO_x conversion increases with the alpha value; however so does the average and maximum ammonia slip. Eventually, at a given alpha value, the NO_x conversion does not change significantly, yet the ammonia slip values continue to increase.

The NO_x conversion performance difference between the 4" and the 8" catalyst is lower for the constant alpha dosing (6.2%), even under significant over-dosing, than when the optimized dosing profiles are used (9.2%). Furthermore, when using the constant alpha dosing strategy, the absolute performance difference changes with the alpha value until there is clear over-dosing. Therefore, the true NO_x conversion performance of the respective catalyst configuration cannot be clearly determined using the constant alpha dosing strategy.

With regards to vehicle application, constant alpha dosing provides less information about the NO_x conversion potential when staying below desired ammonia slip constraints. For example, in the case of the 8" catalyst, a constant alpha of 0.78 satisfies the ammonia slip constraints, but at the same time yields a NO_x conversion that is approximately 9% lower compared to the optimized case. The higher NOx conversion resulting from the optimized look-up table dosing strategy is because this strategy adds the ammonia based on catalyst activity rather than on NO_x concentrations.

2.3.4 Use of Single Look-up Table for Various Driving Cycles

As discussed in Section 2.3.2, the look-up table based dosing strategy described in this work allows for the possibility of applying the optimized table to different conditions, e.g., different driving cycles.

To demonstrate the use of a single look-up table for various driving cycles, the WHTC cycle used in Section 2.3.3.2 was optimized for an 8" long, 12" diameter iron zeolite catalyst for the 50 ppm maximum ammonia slip, 10 ppm average ammonia slip, and the identical hardware and temperature dosing constraints as previously discussed. This optimized look-up table was then used for an ETC and FTP cycle with the identical iron zeolite catalyst, such that the ammonia slip and NO_x conversion could be analyzed. The three selected driving cycles have considerably different input conditions for the SCR, which is demonstrated via the inlet gas temperature profiles in Figure 9.

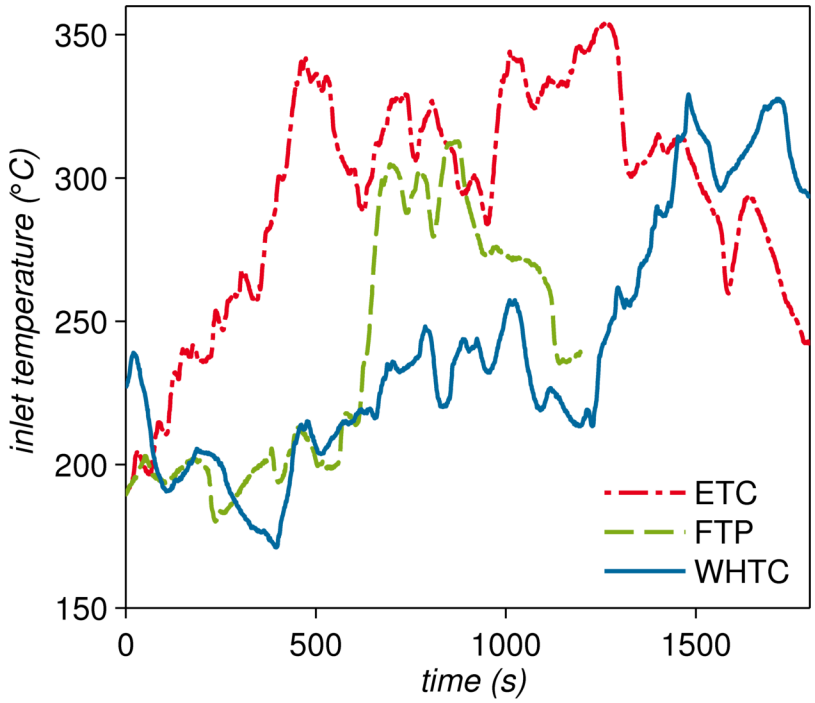

Figure 9. Inlet gas temperature profile for used driving cycles.

The optimization of the entries of the look-up table yields a NO_x conversion of 79.1% and satisfies the constraints when used for the WHTC driving cycle. The optimized table for the WHTC driving cycle was then used for the ETC and FTP driving cycles, where the resulting average ammonia slip, maximum ammonia slip, and NO_x conversion are compared in Table 3.

Table 3. Using optimized WHTC look-up table for ETC and FTP driving cycle.

Cycle	Av. NH_3 slip / ppm	Max. NH_3 slip /.ppm	NO_x conv.	NO_x conv. (opt.)
WHTC	10.0	36.8	79.1%	79.1%
ETC	10.2	51.2	89.2%	89.2%
FTP	7.3	37.4	77.0%	77.6%

In this table, it can be seen that despite the use of the WHTC table, the FTP driving cycle constraints are still satisfied and a NO_x conversion of 77.0% is achieved. Note that when the look-up table is optimized specifically for the FTP cycle, a NO_x conversion of 77.6% is achieved, and the WHTC look-up table conversion comes very close to this value.

The ETC driving cycle's constraints are not exactly satisfied, but are violated by less than 3%. This should be expected, since the driving cycle is much warmer than the optimized WHTC driving cycle and as a result, has a greater sensitivity to the surface coverage values at higher catalyst temperatures. Nevertheless, the values are very close to the upper bounds of the constraints. As the constraints are exceeded slightly, the NO_x conversion (89.2%) is the same as what is achieved when the ETC optimized dosing strategy is used.

Overall, through this comparison, it can be seen that the proposed look-up table optimization approach produces robust dosing strategies for different driving cycles. This robustness is due to the nature of the look-up table, which depends on the catalyst temperature and therefore dictates the ammonia surface coverage.

In the context of real-driving emissions, the proposed look-up table ammonia dosing strategy could be a promising tool for random-cycle testing in the laboratory during catalyst screening and development. Random-cycle testing refers to a test procedure that is composed of short, randomly arranged parts of typical driving conditions [22]. Due to the positive results for the robustness of the look-up table, as demonstrated in

this section, it could be successfully used for various randomly generated driving cycles.

2.4 Conclusions

This work presented a practical, model-based ammonia dosing strategy that maximizes the NO_x conversion while staying within set constraints, in particular ammonia slip constraints, for a given driving cycle. This method can be used in modelling and laboratory environments due to its much lower complexity and short optimization time. Advantages of the method include its ability to handle various constraints and its robustness for other conditions (e.g., driving cycles) due to the look-up table's dependence on the catalyst temperature.

The work also demonstrated the importance of an optimized dosing strategy for each catalytic converter during screening experiments. In this context, a poorer performance was seen when interchanging the dosing profiles for different catalyst materials and volumes as opposed to using its individualized dosing profile. Employing a constant alpha (ppm NH_3/ppm NO_x) dosing strategy also does not show the full catalytic converter potential.

Therefore, determining the optimal dosing strategy of a particular catalytic converter during the development stages allows a benchmark for the best achievable performance. Knowing this best possible performance could assist in decision-making for catalyst materials and system design.

2.5 References

[1] M. Koebel, M. Elsener, M. Kleemann, Urea-SCR: a promising technique to reduce NOx emissions from automotive diesel engines, Catalysis Today 59 (2000) 335-345.

[2] S. Roy, M.S. Hegde, G. Madras, Catalysis for NOx abatement, Appl. Energy 86 (2009) 2283-2297.

[3] D. Peitz, A.M. Bernhard, M. Mehring, M. Elsener, O. Kröcher, Harnstoffhydrolyse für die selektive katalytische Reduktion von NOx: Vergleich der Flüssig- und Gasphasenzersetzung, Chemie Ingenieur Technik 85 (2013) 625-631.

[4] M. Colombo, I. Nova, E. Tronconi, A comparative study of the NH3-SCR reactions over a Cu-zeolite and a Fe-zeolite catalyst, Catalysis Today; Diesel emissions control catalysis 151 (2010) 223-230.

[5] A. Schuler, M. Votsmeier, P. Kiwic, J. Gieshoff, W. Hautpmann, A. Drochner, H. Vogel, NH3-SCR on Fe zeolite catalysts – From model setup to NH3 dosing, Chem. Eng. J. 154 (2009) 333-340.

[6] J.N. Chi, Control Challenges for Optimal NOx Conversion Efficiency from SCR Aftertreatment Systems, - 2009-01-0905 (2009).

[7] F. Willems, R. Cloudt, E. van den Eijnden, M. van Genderen, R. Verbeek, B. de Jager, W. Boomsma, I. van den Heuvel, Is Closed-Loop SCR Control Required to Meet Future Emission Targets?, - 2007-01-1574 (2007).

[8] M. Shost, J. Noetzel, M. Wu, T. Sugiarto, T. Bordewyk, G. Fulks, G.B. Fisher, Monitoring, Feedback and Control of Urea SCR Dosing Systems for NOx Reduction: Utilizing an Embedded Model and Ammonia Sensing, SAE Technical Paper 2008-01-1325 (2008).

[9] A. Güthenke, D. Chatterjee, M. Weibel, B. Krutzsch, P. Kočí, M. Marek, I. Nova, E. Tronconi, Current status of modeling lean exhaust gas aftertreatment catalysts, in: Guy B. Marin (Ed.), Advances in Chemical Engineering, Academic Press, 2007, pp. 103-283.

[10] E.N. Fuller, P.D. Schettler, J.C. Giddings, A new method for prediction of binary gas-phase diffusion coefficients, J. Ind. Eng. Chem. 58 (1966) 18-27.

[11] E. Tronconi, P. Forzatti, Adequacy of lumped parameter models for SCR reactors with monolith structure, AIChE Journal 38 (1992) 201-210.

[12] W. Hauptmann, M. Votsmeier, H. Vogel, D.G. Vlachos, Modeling the simultaneous oxidation of CO and H2 on Pt - Promoting effect of H2 on the CO-light-off, Appl. Catal., A 397 (2011) 174-182.

[13] S. Malmberg, M. Votsmeier, J. Gieshoff, N. Soeger, L. Mussmann, A. Schuler, A. Drochner, Dynamic phenomena of SCR-catalysts containing Fe-exchanged zeolites - experiments and computer simulations, Topics in Catalysis 42-43 (2007) 33-36.

[14] D. Chatterjee, T. Burkhardt, M. Weibel, I. Nova, A. Grossale, E. Tronconi, Numerical Simulation of Zeolite- and V-Based SCR Catalytic Converters, SAE Technical Paper 2007-01-1136 (2007).

[15] D. Chatterjee, P. Koci, V. Schmeisser, M. Marek, M. Weibel, B. Krutzsch, Modelling of a combined storage and -SCR catalytic system for Diesel exhaust gas aftertreatment, Catalysis Today 151 (2010) 395-409.

[16] M. Colombo, I. Nova, E. Tronconi, V. Schmeisser, B. Bandl-Konrad, L. Zimmermann, NO/NO2/N2O-NH3 SCR reactions over a commercial Fe-zeolite catalyst for diesel exhaust aftertreatment: Intrinsic kinetics and monolith converter modelling, Applied Catalysis B: Environmental 111-112 (2012) 106-118.

[17] A. Scheuer, W. Hauptmann, A. Drochner, J. Gieshoff, H. Vogel, M. Votsmeier, Dual layer automotive ammonia oxidation catalysts: Experiments and computer simulation, Applied Catalysis B: Environmental 111–112 (2012) 445-455.

[18] W. Hauptmann, A. Schuler, J. Gieshoff, M. Votsmeier, Modellbasierte Optimierung der Harnstoffdosierung für SCR-Katalysatoren, Chemie Ingenieur Technik 83 (2011) 1681-1687.

[19] S. Samuel, L. Austin, D. Morrey, Automotive test drive cycles for emission measurement and real-world emission levels - a review, Proceedings of the Institution of Mechanical Engineers, Part D: Journal of Automobile Engineering 216 (2002) 555-564.

[20] T.J. Barlow, S. Latham, I.S. McCrae, P.G. Boulter, A reference book of driving cycles for use in the measurement of road vehicle emissions PPR354 (2009).

[21] A.M. Bernhard, D. Peitz, M. Elsener, T. Schildhauer, O. Kroecher, Catalytic urea hydrolysis in the selective catalytic reduction of NOx: catalyst screening and kinetics on anatase TiO2 and ZrO2., Catalysis Science & Technology 3 (2013) 942-951.

[22] M. Weiss, P. Bonnel, R. Hummel, N. Steininger, A complementary emissions test for light-duty vehicles: Assessing the technical feasibility of candidate procedures EUR 25572 EN (2013).

Chapter 3 - Comparison of SCR and SCR + ASC Performance: A Simulation Study

A version of this chapter will be submitted to a peer-reviewed journal.

Meeting the more stringent, government-imposed exhaust emission standards that result in more challenging driving cycles, as well the possibility of using Real Driving Emissions in future regulations, present a significant challenge in the development of efficient exhaust after-treatment systems [1]. Selective catalytic reduction (SCR) has been, and currently is, the method of choice in attaining the demanding NO_x regulations for diesel vehicles emissions, at least for larger engines [2, 3]. This approach operates under the principle that ammonia, the reducing agent, is generated onboard through the hydrolysis of urea and is injected into the SCR according to a chosen dosing strategy. Ammonia can be adsorbed or desorbed by the SCR catalyst, which is beneficial when too much has been dosed or more is needed to convert the NO_x gas [4]; however, the storage capacity of ammonia in the catalyst decreases strongly with an increase in temperature [2]. This means that a sharp increase in load and engine, e.g. due to acceleration, can result in a significant amount of ammonia slip. Therefore, a well-designed catalytic converter and operating strategy must be developed, such that the NO_x conversion is maximized, while maintaining the ammonia slip below a currently non-regulated acceptable level.

In terms of catalytic converter design, there is the possibility of adding an ammonia slip catalyst (ASC) as a short zone directly after the SCR to convert the ammonia exiting the SCR-zone to nitrogen. The ASC is able to increase the conversion of ammonia through its ammonia oxidation layer (AOC), which uses a platinum catalyst on a supported oxide. Where the platinum catalyst has a poor selectivity to nitrogen at higher temperatures, resulting in NO_x formation from the ammonia oxidation, a dual layer concept consisting of a lower AOC layer and an upper SCR layer is used to increase the ASC's selectivity to nitrogen [5].

Numerical simulation is an important tool for the development of these exhaust after-treatment systems, particularly where physical experiments are very time consuming and costly [6]. In this context, the SCR has been well-modelled and the literature provides a good overview [3, 7-10]. Likewise, models for the ASC have recently been published and have been used for analyses of the ASC design. For instance, Scheuer et al. [5] used their published, experimentally-validated numerical model to complete a design parameter study (SCR layer washcoat loading, diffusion coefficient, catalyst size) for the ASC. In the process of developing and validating an ASC model, Colombo et al. [11, 12] compared steady state operations between dual-layer and mixed ASCs, where the powders of the two different layers are mixed as a single layer. Shrestha et al. [13] also experimentally investigated the performance of a dual-layer and mixed ASC; however, at different space velocities and reactant compositions to examine their effect on ammonia oxidation and N_2 selectivity. Kamasamduram et al. [14] used progressive catalyst aging to understand the degradation of the ASC and make comparisons to a diesel oxidation catalyst (DOC)

and SCR. Although analyses of both the SCR and ASC have been completed, to our knowledge, a simulation study of adding an ASC after an SCR during driving cycles has yet to be investigated. This design set-up could assist in meeting the demanding driving cycles due to the ASC's ability to oxidize the ammonia, consequently reducing the ammonia slip and potentially allowing for a higher NO_x conversion through more aggressive ammonia dosing.

Therefore, in this work, performance comparisons (NO_x conversion, ammonia slip) between an SCR and an SCR with an ASC addition are presented. These comparisons provide a better understanding of the value of an ASC throughout driving cycles and in particular, its impact on the overall system's NO_x conversion and ammonia slip. This investigation was done using the experimentally validated ASC model of [5]. To begin, the base performance of the two catalytic converter designs was first investigated and compared through steady state tests at different temperatures and a system response test to a sudden increase in temperature. Thereafter, driving cycles were used, and the optimized dosing strategy presented in Chapter 2 was applied to make meaningful comparisons between the catalytic converter designs under transient inputs; the knowledge gained in the base performance review assisted in understanding the catalytic converter response. Overall, an ASC's benefit in meeting the regulatory requirements during the demanding test cycles is shown.

3.1 Models

In this work, two different catalyst layouts were used and are compared. The first catalyst design used throughout this simulation study consisted of an 8" SCR catalyst.

The second design had a front-end SCR and a back-end ASC. The length of the SCR varied based on the length of the ASC such that the combined monolith length is 8". A schematic of both catalytic converter layouts can be seen in Figure 10. Where a dual-layer ASC is used, the upper SCR layer had the same washcoat loading as the 8" SCR. Both of these systems had a diameter of 12", a density of 400 cpsi, and a wall thickness of 6.5 mil.

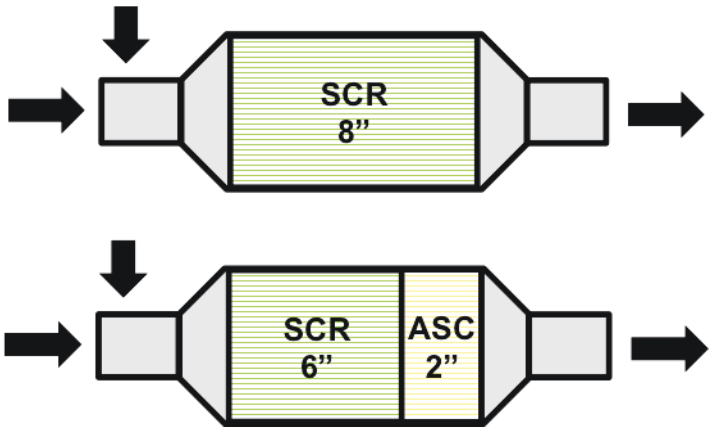

Figure 10. Catalytic Converter Layouts Used.

Single channel models are used to describe the behavior of the exhaust gas passing through both the SCR and the ASC. As the geometrical properties of the channels, their catalyst distribution, and the inlet conditions are assumed identical, the model is assumed to be representative of each channel in the reactor. A 1D model is used for simulation of the SCR channels, whereas a 1D + 1D model is used for the ASC. Both of these models were developed and provided by Umicore AG & CO. KG and are briefly described in the following subsections for completeness.

3.1.1 SCR Model

In the one-dimensional SCR model, the temperature and concentration variations in the radial direction are neglected and are assumed to be mixing cup values (lumped parameters). Equations (1) and (2) describe the mass balances for the gas phase and the gas in the washcoat, respectively. Equation (1) accounts for the axial convection and mass transfer from the gas phase to the washcoat, and Equation (2) also accounts for the mass transfer and the reaction in the specific washcoat layer.

$$\frac{\partial c_{gas,i}}{\partial t} = -v_{gas} \cdot \frac{\partial c_{gas,i}}{\partial z} - \beta_i \cdot \frac{4}{D_H} \left(c_{gas,i} - c_{wc,i}\right) \tag{1}$$

$$\frac{dc_{wc,i}}{dt} = \Phi \cdot \beta_i \cdot \left(c_{gas,i} - c_{wc,i}\right) + \sum_j \left(v_{i,j} \cdot r_j\right) \tag{2}$$

In the equations above, c_{gas} and c_{wc} represent the concentration of the gas *i* and the gas species *i* in the washcoat phase, respectively and z represents the axial position in the reactor. Additionally, the variable v_{gas} represents the average gas velocity, D_H is the hydraulic diameter, β_i represents the position dependent mass transfer coefficient (calculated via equations (4) and (5) in Chapter 2), and Φ is a geometrical factor for the specific surface area between the gas and solid phase per washcoat volume.

Equations (3) and (4) describe the energy balances for the gas phase and gas in the washcoat. Equation (3) accounts for convection and the heat added to the gas from the surface. Equation (4) accounts for the heat transferred from the solid to the gas as well as the heat released from the reaction.

$$\frac{\partial T_{gas}}{\partial t} = -v_{gas} \cdot \frac{\partial T_{gas}}{\partial z} - \alpha \cdot \frac{4}{D_H \cdot \rho_{gas} \cdot c_{p,gas}} \cdot (T_{gas} - T_{wc}) \quad (3)$$

$$\frac{dT_{wc}}{dt} = \alpha \cdot \frac{4}{D_H \cdot \rho_{wc} \cdot c_{p,wc}} \cdot (T_{gas} - T_{wc}) + \frac{\sum_j (\Delta H_j \cdot r_j)}{\rho_{wc} \cdot c_{p,wc}} \quad (4)$$

In the equations above T_{gas} represents the gas temperature and T_{wc} represents the temperature of the washcoat. Additional definitions of variables include ρ, which the density, c_p is the heat capacity, ΔH_j is the reaction enthalpy, and r_j is the reaction rate.

The system of equations were solved numerically for each volume element. More detail regarding the reactor model has been given in Chapter 2 and can be found in [15].

The SCR kinetic model was previously published in [7]. The mechanistic model was parameterized using steady state and transient data, and takes into account the following global reactions:

Adsorption/Desorption $NH_3 + [*] \leftrightarrow NH_3*$ (R4)

Standard SCR: $4NH_3 + 4NO + O_2 \rightarrow 4N_2 + 6H_2O$ (R5)

Fast SCR: $4NH_3 + 2NO + 2NO_2 \rightarrow 4N_2 + 6H_2O$ (R6)

NO_2 SCR: $8NH_3 + 6NO_2 \rightarrow 7N_2 + 12H_2O$ (R7)

Ammonia Oxidation: $4NH_3 + 3O_2 \rightarrow 2N_2 + 6H_2O$ (R8)

NO Oxidation: $NO + 0.5 \leftrightarrow NO_2$ (R9)

For more details regarding the reaction mechanism, see Schuler et al. [7].

3.1.2 ASC Model

The ASC consists of an upper SCR layer and a lower ammonia oxidation layer and is typically added as a short zone after the SCR. Where the ASC must generally operate close to the mass transfer limit, radial diffusion effects in the washcoat must be considered and therefore a 1D + 1D model was used [16].

Hence, as completed with the SCR model, Equation (1) and (3) are used to describe the concentration and temperature behavior of the exhaust gas through the ASC. For every lumped parameter gas phase position solved in the axial direction, a one-dimensional concentration and temperature profile is solved for in the radial direction for the two layers. The radial concentration is solved for in Equation 5 and its boundary condition is shown is Equation (6).

$$\frac{\partial c_{wc,i}}{\partial t} = \frac{\partial J_{wc,i}}{\partial x} + r_j \quad \text{with} \quad J_{wc,i} = -D_{eff,i} \cdot \frac{\partial c_{wc,i}}{\partial x} \tag{5}$$

$$D_{eff,i} \cdot \left. \frac{dc_{wc,i}}{dx} \right|_{x=0} = \beta_i \cdot (c_{wc,i}|_{x=0} - c_{gas,i}) \tag{6}$$

In Equations (5) and (6), the variable $D_{eff,i}$ represents the diffusion coefficient of species *i* in the washcoat and $J_{wc,i}$ is the flux of the *i* along the radial coordinate x. The radial temperature profile is solved for via Equation (7). In this equation, the variable d_{wc} represents the washcoat thickness.

$$\frac{dT_{wc}}{dt} = \Phi \cdot \frac{\alpha}{\rho_{wc} \cdot c_{p,wc}} \cdot (T_{gas} - T_{wc}) + \Phi \cdot \frac{1}{\rho_{wc} \cdot c_{p,wc}} \cdot \int_0^{d_{wc}} \Delta H_j \cdot r_j \cdot dx \tag{7}$$

Owing to the ASC's dual-layer structure, two different kinetic models are used for the ASC. The SCR kinetic model briefly outlined in Section 3.1.1 was used for the SCR

and the AOC kinetic model described here is used for the lower ammonia oxidation layer. Therefore, the following ammonia oxidation catalyst global reactions were accounted for in this model:

$$4NH_3 + 3O_2 \rightarrow 2N_2 + 6H_2O \quad \text{(R10)}$$

$$2NH_3 + 2O_2 \rightarrow N_2O + 3H_2O \quad \text{(R11)}$$

$$NH_3 + 2O_2 \rightarrow NO_2 + 1.5H_2O \quad \text{(R12)}$$

$$NH_3 + 2O_2 \rightarrow NO_2 + 1.5H_2O \quad \text{(R13)}$$

$$2NH_3 + 2NO + 1.5O_2 \rightarrow 2N_2O + 3H_2O \quad \text{(R14)}$$

$$NO + 0.5 \leftrightarrow NO_2 \quad \text{(R15)}$$

$$2NH_3 + 2NO_2 + 0.5O_2 \rightarrow 2N_2O + 3H_2O \quad \text{(R16)}$$

The mechanistic model used was previously published in [5] and was parameterized using a variety of experimental data at collected at different inlet conditions. It was assumed that the kinetics are not influenced by internal mass transfer limitations. In [18] it was shown that the diffusion effects could be neglected at washcoat loadings below 25 g/L. Therefore, where the washcoat loading in this study were below this value, this model could be used.

3.2 Ammonia Dosing Strategy

Comparisons between the catalytic converter configurations were completed under steady state (Sections 3.3.1 and 3.3.2) and transient conditions (Sections 3.3.3 and 3.3.4). The comparisons at steady state were completed under constant input conditions that are specified in their corresponding sections. Transient condition comparisons were completed using the WHTC driving cycle. Although the engine

speed and load are specified for the WHTC driving cycle [15], the input data used for the catalytic converter designs were experimental values from the test bench once the exhaust gas has passed through a Diesel Oxidation Catalyst (DOC) and a Catalyzed Diesel Particle Filter (CDPF). This means that only the SCR or SCR + ASC needs to be considered in all of the simulation study experiments.

To make meaningful comparisons between the catalytic converters during transient conditions, an optimal ammonia dosing strategy must be considered [16]. Therefore, Section 3.3.3 and 3.3.4 use an optimized ammonia dosing strategy to evaluate the catalyst performance over a given driving cycle. This dosing strategy is briefly described here, but the reader is encouraged to refer to Chapter 2 for more information.

The ammonia dosing strategy achieves its goal for a given driving cycle, e.g. maximizing NO_x while fulfilling the ammonia slip constraints, according to a look-up table that has been optimized for the given driving cycle. This optimized look-up table is essentially a piece-wise function that takes into account the catalyst activity by relating the catalyst temperature to a desired ammonia surface coverage.

Figure 11 will assist in explaining how the optimized look-up table is used for the dosing strategy, which can be described in the following three steps, which can be completed successively for each time instance of a given driving cycle:

1) At a given time instant (t), ammonia ($n_{NH3,in}(t)$) is injected into the exhaust gas stream in front of the catalyst. At this time instant, the SCR model is used to

calculate the output variables including the average catalyst temperature ($T_{cat.}(t)$) and actual average ammonia surface coverage ($\Theta_{act.}(t)$).

2) The look-up table is then used to determine the setpoint, or desired average ammonia surface coverage ($\Theta_{des.}(t)$), for the current catalyst temperature via linear interpolation between table entries.

3) The amount of ammonia required for the actual surface coverage to reach the desired can then be calculated via:

$$n_{\mathrm{NH_3in}(t+\Delta t)} = \begin{cases} [\Theta_{des.}(t) - \Theta_{act.}(t)] \cdot \sigma \cdot V, & \text{if } \Theta_{des.}(t) > \Theta_{act.}(t) \\ 0, & \text{otherwise} \end{cases} \quad (8)$$

where $\Theta(t)$ represents the average ammonia surface coverage, σ the number of active sites per reactor volume and V the catalyst volume.

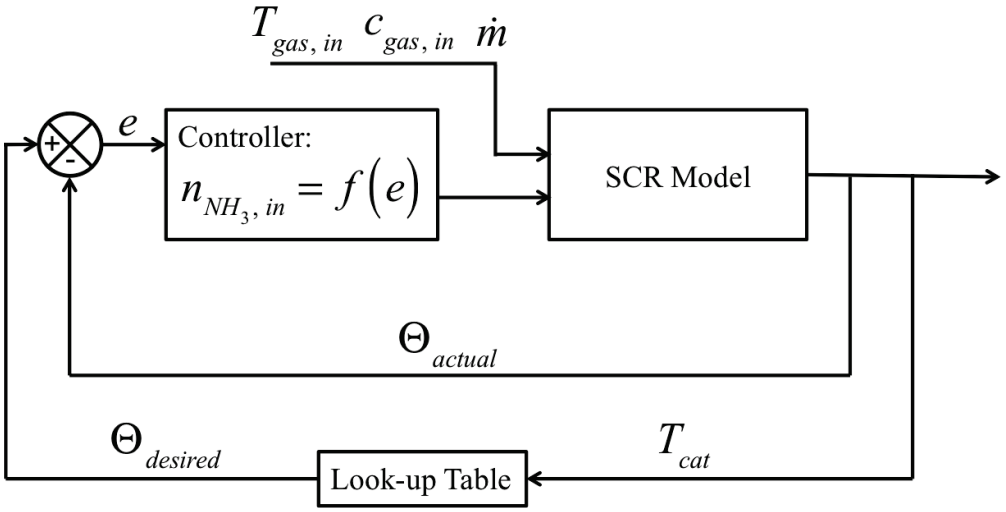

Figure 11. Schematic of Dosing Strategy.

The optimization of the look-up table's entries is completed through the following summarized steps:

1) Adjusting the look up table entry values via an optimization algorithm.

2) Using the look-table for the ammonia dosing control in the simulation with a given driving cycle (Figure 11).
3) Calculating the resulting objective function and constraint values from Step 2.

These steps are repeated until the change in the objective function was below a specified tolerance.

3.3 Results & Discussion

The following two subsections compare the performance between an 8" SCR catalytic converter and a catalytic converter configuration consisting of a 6" SCR with a 2" ASC using constant alpha (NH_3/NO_x ratio) dosing experiments for constant input gas compositions. Its purpose is to better understand the ASC's behavior and establish its benefit through steady state simulation experiments.

3.3.1 System Performance Analysis at Different Alpha Values

For this particular simulation study, ammonia was added to the catalytic converter configuration based on the specified alpha value, and the stationary NO_x conversion and ammonia slip are recorded once the system has reached steady state. This was completed for many different alpha values and allows one to observe how the NO_x conversion and ammonia slip leaving the converter changes with ammonia added. The inlet gas feed was at a constant space velocity of 30,000 h^{-1} and had a mole fraction composition of 420 ppm NO, 180 ppm NO_2, 5% O_2, and 5% H_2O. As the ammonia added varies based on the specified alpha ratio, the N_2 acts as the mole fraction balance. This was completed for two different inlet gas temperatures, 200°C and 300°C.

Each converter configuration's change in NO_x conversion and ammonia slip with alpha at the specified temperature can be seen in Figure 12 and 13. When analyzing the upper two graphs corresponding to an inlet temperature of 200°C, one can note that at alpha values less than approximately 0.60, there is almost no ammonia slip leaving both catalytic converters (Figure 12 – right). As the alpha value increases from 0.50 to 0.60, the NO_x conversion increases identically for both systems because both systems have complete ammonia conversion (Figure 12 – left).

At an inlet gas temperature of 200°C and alpha values greater than approximately 0.60, the ammonia conversion for the catalytic converters decreases. This decrease in ammonia conversion can be realized because the ammonia slip rises and the NO_x conversion and ammonia slip values differ between the two systems (SCR vs. ASC). Through the graphs, it can be seen that the SCR + ASC achieves higher NO_x conversion values compared to the 8" SCR because of the conversion of ammonia and NO_x to N_2O, a strong greenhouse gas [19], in the ASC system. Likewise, for every alpha value, the SCR + ASC has less ammonia slip. In both cases, the ammonia added to both of the converters eventually no longer increases the NO_x conversion and, as a result, the ammonia slip values rise steeply with the alpha value. Most importantly, it can be concluded that at this temperature, the SCR + ASC demonstrates a better overall performance compared to the SCR system.

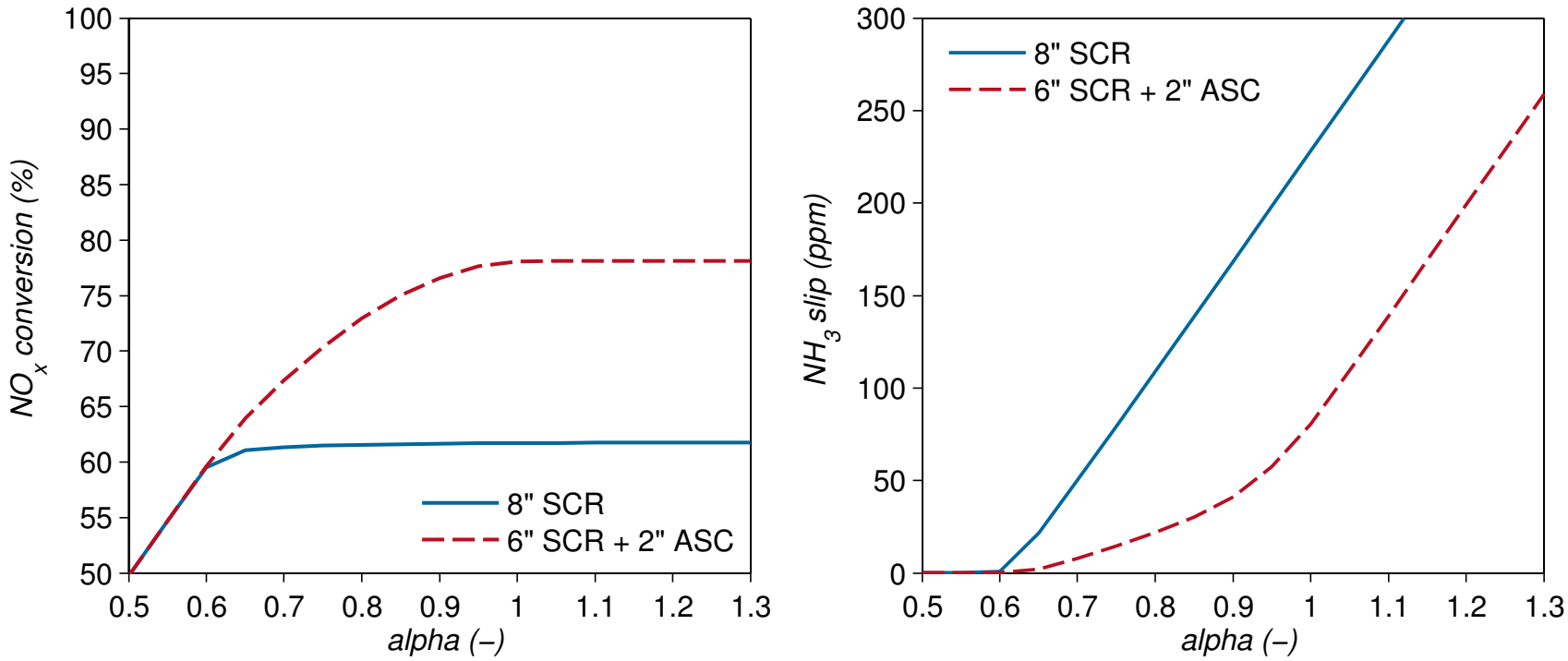

Figure 12. NO_x conversion and ammonia slip for an 8" SCR and a 6" SCR with a 2" ASC zone during steady state alpha dosing simulation experiments at 200°C.

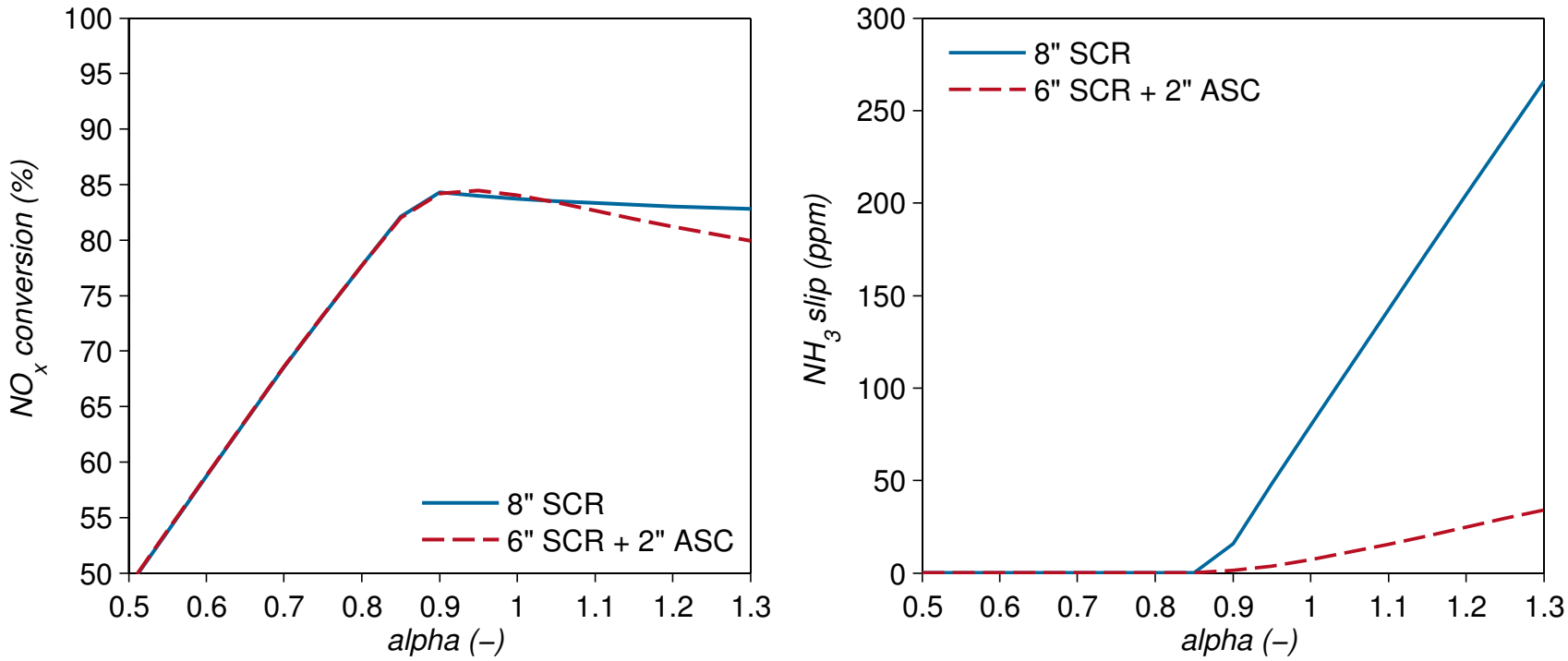

Figure 13. NO_x conversion and ammonia slip for an 8" SCR and a 6" SCR with a 2" ASC zone during steady state alpha dosing simulation experiments at 300°C.

The same effects can be seen for the catalytic converter behaviors at an inlet gas temperature of 300°C (Figure 13) and an alpha value less than 0.85 when ammonia is being completely converted in the respective converter configuration (e.g. the ASC); however, at alpha values above 0.85, a slightly different behavior occurs. Again, the SCR + ASC system has less ammonia slip due to the ASC's ability to oxidize the ammonia exiting the SCR brick; yet, the NO_x conversion also does not exceed the SCR's NO_x conversion for any alpha value. This occurs as the excess ammonia is being oxidized to NO_x in the ASC, which occurs at higher temperatures. The NO_x conversion also decreases slightly with increasing alpha for the SCR system because of the inhibition of ammonia.

In short, at the given inlet conditions, it can be seen that the deNOx performance for the SCR + ASC system at higher alpha values is dependent upon the inlet temperature of the gas. Lower inlet gas temperatures (e.g., 200°C) allowed for a more significant deNOx performance for the SCR + ASC catalytic converter because of the ASC base's higher selectivity for nitrogen and N_2O. Higher inlet gas temperatures (e.g., 300°C) also allowed for less ammonia slip with little NO_x conversion loss.

3.3.2 System Response to Step Increase in Inlet Gas Temperature

Temperature step simulation experiments are completed in this section to be able to analyze and compare the catalytic converter's response, in particular ammonia slip breakthrough. Therefore, a constant amount of ammonia was added to each configuration such that both systems had the same amount of ammonia slip once steady state was reached. Thereafter, a step increase in the inlet gas temperature from

200ºC to 300ºC was implemented while the ammonia supplied to the system was simultaneously cut off. As in the previous section, the inlet gas space velocity used was 30,000 h^{-1} and has a mole fraction composition of 420 ppm NO, 180 ppm NO_2, 5% O_2, and 5% H_2O.

To achieve a steady state ammonia slip of 10 ppm at the specified inlet conditions, ammonia was added at an alpha ratio of 0.63 for the SCR and 0.72 for the SCR + ASC system. Figure 14 shows the inlet gas temperature, inlet amount of ammonia, the resulting ammonia slip, and the resulting amount of NO_x gas exiting the two different catalytic converter designs over time. In this figure, it can be seen that before 500 s, the converters are at steady state and both have 10 ppm ammonia slip.

Before 500 s, the stationary NO_x conversion for the SCR is 60.8% and 68.4% for the SCR + ASC. A higher NO_x conversion is achieved for the SCR + ASC system because ammonia slip and NO_x exiting the 6" SCR zone is being converted to N_2O, as highlighted in Section 3.3.1. As more ammonia can be converted over this 2" ASC zone compared to the last 2" of the SCR, a higher alpha value is added to the SCR + ASC system.

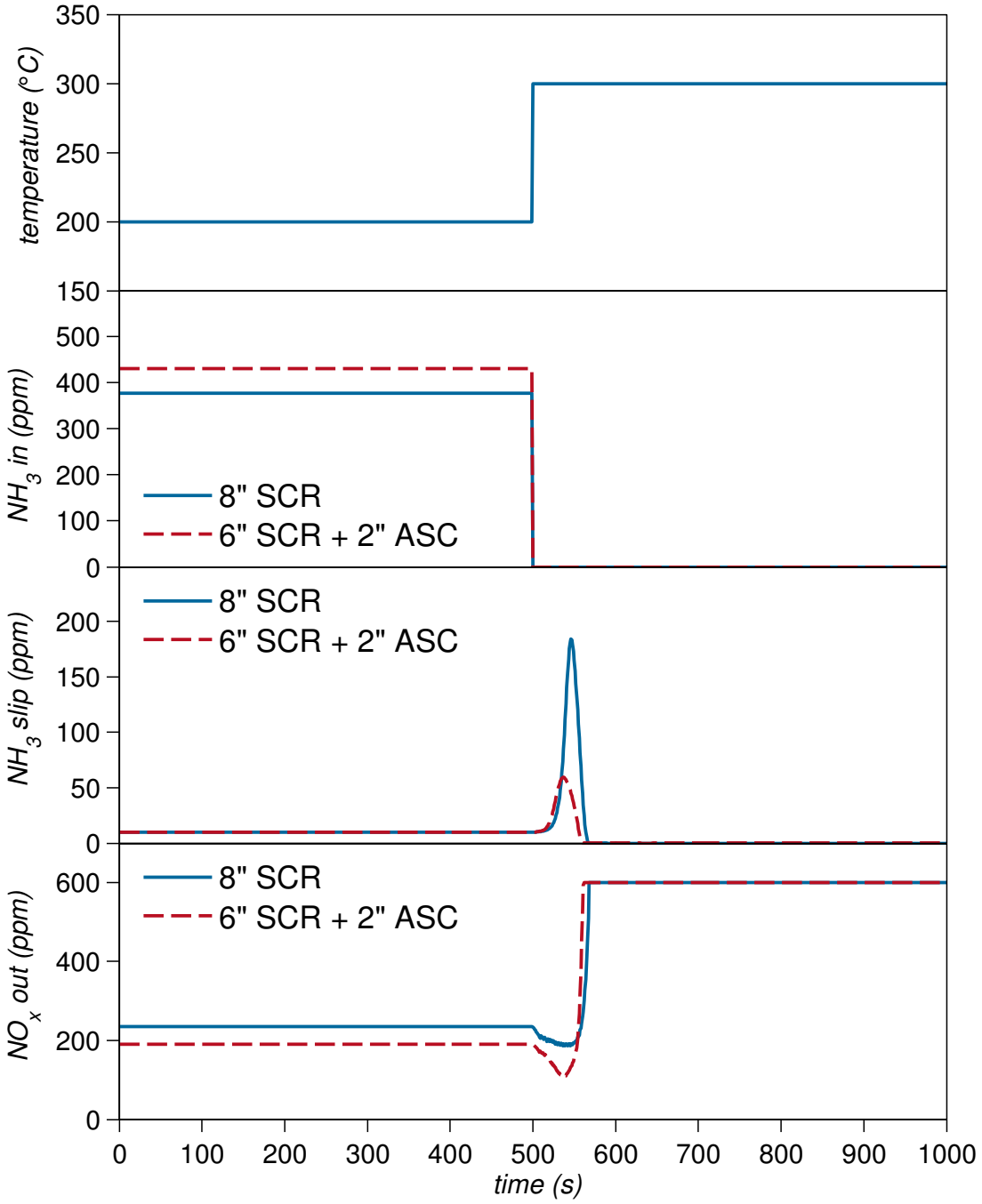

Figure 14. Comparison of system response (ammonia slip, outlet NO_x) to an initial step change in temperature for an 8" SCR and a 6" SCR with a 2" ASC zone at 30,000 h^{-1}.

When an inlet gas temperature increase of 100ºC occurs and the ammonia supplied is simultaneously cut off, one can see through Figure 14 that the SCR + ASC system

response results in approximately a third of the amount of ammonia slip compared to the SCR. Less ammonia slip arises from the SCR + ASC system as the ASC-brick is able to oxidize the ammonia.

If the same experiments were to be completed at a very high space velocity (e.g., 120,000 h^{-1}), one would observe that approximately the same amount of ammonia, or alpha values, would be added to the 8" SCR as for the 6" SCR + 2" ASC. This occurs because the ASC layer is not accessible owing to the diffusion limitation in the upper SCR washcoat layer. Likewise, the two catalytic converter configurations' resulting steady state NO_x conversion and the resulting ammonia slip due to the temperature step change would be almost identical.

3.3.3 Comparing Optimized Dosing Profiles for SCR and SCR + ASC System

In this section, the performance of the 8" SCR and combined 6" SCR + 2" ASC system are compared during transient conditions by using the WHTC driving cycle. The purpose of these comparisons is to investigate the benefit of the ASC addition during more realistic driving scenarios.

To make meaningful comparisons between the catalytic converter designs over the driving cycle, the ammonia dosing profile for the 8" SCR was optimized using the strategy presented in Chapter 2 for the WHTC driving cycle. The goal of the ammonia dosing strategy was to maximize the NO_x conversion over the driving cycle while maintaining the average ammonia slip across the driving cycle below 10 ppm and the maximum ammonia slip below 50 ppm. Likewise, the following two additional constraints were included in the model: ammonia could only be added to

the system at any given time instant where the inlet temperature is above 180ºC to ensure the hydrolysis of urea; the maximum amount of ammonia that could be added at any given time instance is 2000 ppm to reflect equipment limitations. The optimization procedure is discussed in more detail in the Section 3.2 or in Chapter 2.

The ammonia dosing strategy was first optimized for an 8" SCR during the WHTC driving cycle. When using this strategy for the 8" SCR during the WHTC driving cycle, a NO_x conversion of 79.1% was achieved; this result can be seen in Table 4.

Next, the identical SCR optimized dosing profile was applied to a 6" SCR + 2" ASC system, such that the same amount of moles of ammonia were added at every time instant as was done for the SCR. It was expected that the amount of ammonia slip from the catalytic converter system would decrease, as the ASC's oxidation layer is able to convert the ammonia. Ideally, the additional conversion of ammonia would result in a greater selectivity to nitrogen, which would increase the overall NO_x conversion. The results of applying the dosing profile to the 6" SCR and 2" ASC system (Table 4) show that the ammonia slip exiting the catalytic converter did indeed decrease; however, the NO_x conversion remained approximately the same.

Table 4. Applying Ammonia Dosing Strategy for Catalytic Converter Designs during WHTC Driving Cycle

	Target	Opt. 8" SCR	6" SCR + 2" ASC	Opt. 6" SCR + 2" ASC
NO_x Conv. (%)	maximize	79.1	78.9	82.1
Avg. NH_3 Slip (ppm)	≤ 10	10.0	2.1	10.0
Max. NH_3 Slip (ppm)	≤ 50	36.8	22.8	50.0
Moles NH_3 Added (mol)	-	5.33	5.33	6.04

Finally, the benefit of an ASC is investigated by optimizing the ammonia dosing profile for the 6" SCR + 2" ASC. It has frequently been stated that the addition of an ASC would allow for more aggressive dosing of ammonia and as a result, increase the overall system's NO_x conversion. This was investigated by comparing the NO_x conversion of the optimized 8" SCR operation strategy over the transient driving cycle to the optimized 6" SCR + 2" ASC operation strategy; as seen in Table 4 the optimized 6" SCR + 2" ASC achieves a slightly higher NO_x conversion (3% increase). Likewise, it can be noted that overall more moles of ammonia are added to the system in comparison to the SCR.

3.3.4 Over/Under-dosing

To investigate further the benefit of an ASC addition during a driving cycle, the individually optimized dosing profile for both the 8" SCR and 6" SCR + 2" ASC system was used and a constant dosing error was introduced to the respective system's optimized dosing profile. Therefore, the catalytic converter's behavior could

be analyzed during constant under- and over-dosing of an optimized dosing profile for a given driving cycle.

The concept of applying constant under- and over-dosing to the catalytic converter designs can be further explained through the assistance of Figure 15. In this figure, an excerpt of the ammonia dosing profile for the 8" SCR catalyst during the WHTC driving cycle, from 1500 seconds to 1700 seconds, is shown. The line representing the "Error in Dosing = 0%" is the optimized dosing profile for the 8" SCR. The lines for the "Error in Dosing = ±20%" represents when a constant 120% or 80% of the ammonia of the optimized dosing profile are added at every time instance, thus introducing a constant error. It is important to note that during the over-dosing cases, it was ensured that the equipment constraint (no more than 2000 ppm of ammonia added at any time instance) was still fulfilled at each time instance; therefore, the total amount of ammonia added over the driving cycle multiplied by the error in dosing is not necessarily the equivalent amount of ammonia added in the over-dosing case.

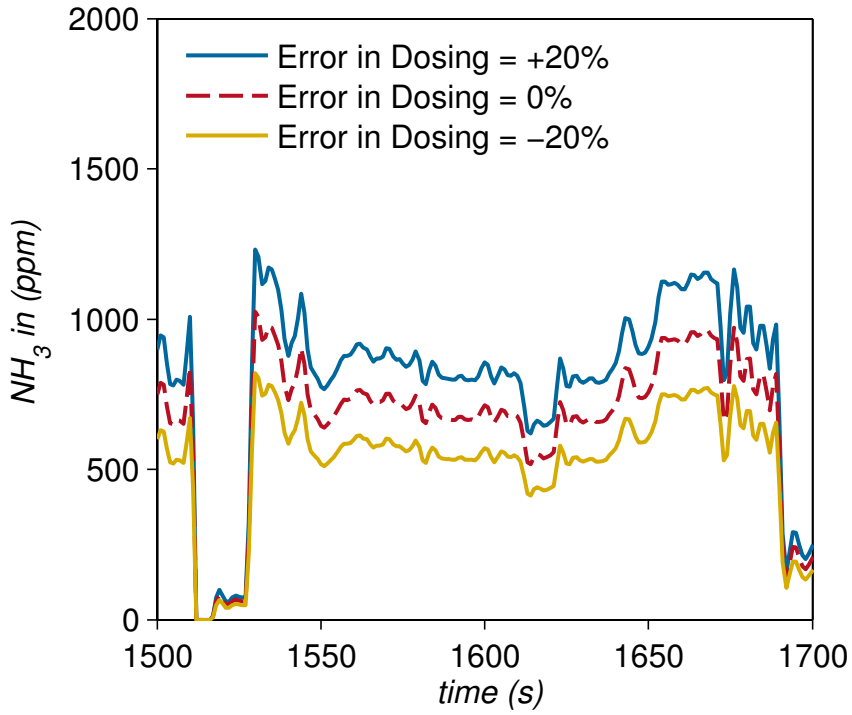

Figure 15. Optimized dosing profile and constant error in dosing profile for an 8" SCR Fe-Zeolite catalyst during the WHTC driving cycle.

A constant error in dosing from the optimum profile, ranging from -20% to +50%, was implemented to the 8" SCR and 6" SCR + 2" ASC during the WHTC driving cycle. The resulting NO_x conversion and ammonia slip values over the simulated driving cycles were calculated for the respective under- and over-dosing scenario. The results are shown in Figure 16.

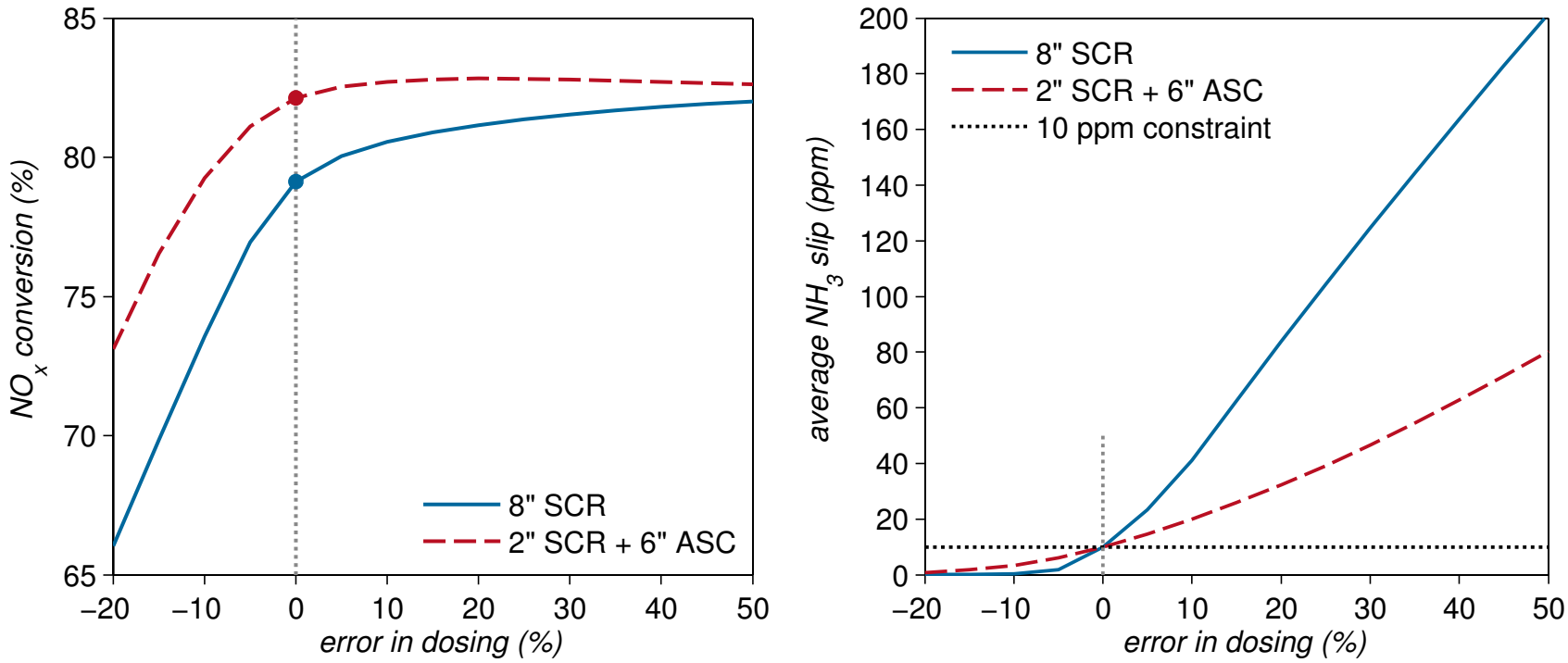

Figure 16. NO_x Conversion and Average Ammonia Slip for different errors in dosing for the WHTC driving cycle.

The NO_x conversions and average ammonia slip values at a 0% error in dosing in Figure 16 represent the optimized result for the respective catalytic converter design. Again, it can be seen that when optimizing the ammonia dosing profile for the respective design, the combined 6" SCR + 2" ASC achieves a slightly higher NO_x conversion than the 8" SCR because, as discussed in Section 3.3.1, ammonia and NO_x leaving the SCR-brick are forming N_2O in the ASC.

When constantly under-dosing ammonia throughout the driving cycle, resulting in a negative error in dosing, the combined SCR + ASC system has a higher NO_x conversion compared to the SCR system, as seen in Figure 16. The higher ammonia slip and NO_x conversion during under-dosing for the SCR + ASC system arises because more moles of ammonia are still being added, which can react in the SCR and form N_2O in the ASC, compared to the SCR.

The NO_x conversion rises marginally and then eventually begins to slightly decrease for the SCR + ASC system when over-dosing ammonia, which corresponds to the positive "error in dosing" values in Figure 16. The NO_x conversion for the 8" SCR continues to rise noticeably. A decrease in NO_x conversion, for the 8" SCR due to the inhibition of ammonia is not seen because not enough ammonia is being added to the system.

Most importantly, when comparing the average ammonia slip for the two different configurations during over-dosing in Figure 16, one can note that significantly more ammonia slip is occurring for the 8" SCR in comparison to the 6" SCR + 2" ASC

system. This again reveals the ASC's ability to oxidize more ammonia, as also discussed and shown in the base performance review (Section 3.3.1).

Finally, this analysis demonstrates the ASC's ability to offer significant security to the exhaust emission after-treatment system when an error in dosing occurs. This could be seen through its capability in maintaining the ammonia slip closer to an acceptable level when over-dosing and allowing for a higher NO_x conversion when under-dosing. The security is particularly beneficial in catalyst aging or unpredictable driving conditions when inadequate amount of ammonia may be added and is not achieved with solely an 8" SCR.

3.4 Conclusions

In this simulation study, an 8" SCR design and a 6" SCR + 2" ASC design were compared in terms of system performance, in particular NO_x conversion while staying under ammonia slip constraints. Through evaluation of the catalytic converters' base performance through constant input tests, it was demonstrated that the SCR + ASC allows for a greater NO_x conversion at lower temperatures (200°C). Furthermore, the SCR + ASC exhibits less ammonia slip at lower and higher temperatures (200°C & 300°C). When both systems are at steady state and have the same amount of ammonia slip and a temperature step increase is introduced, the SCR + ASC has less ammonia slip compared to the SCR.

Through comparisons of the catalytic converter designs with optimized dosing strategies for the WHTC driving cycle, it was also seen that the ASC allows for a slightly higher NO_x conversion. Most importantly, the ASC also acts as a buffer for

over-dosing as it allows for less ammonia slip breakthrough, while during under-dosing it still allows for a greater NO_x conversion compared to only the SCR.

Overall, it can be concluded that the ASC is a positive addition to the SCR in meeting the exhaust emission regulations. Although it does not necessarily allow for a higher NO_x conversion, its ability to cope with under- and over-dosing situations can be beneficial in catalyst aging and unpredictable driving conditions.

3.5 References

[1] M. Weibel, V. Schmeißer, F. Hofmann, Model-Based Approaches to Exhaust Aftertreatment System Development, in: I. Nova, E. Tronconi (Eds.), Springer New York, 2014, pp. 691-707.

[2] M. Koebel, M. Elsener, M. Kleemann, Urea-SCR: a promising technique to reduce NOx emissions from automotive diesel engines, Catalysis Today 59 (2000) 335-345.

[3] I. Nova, E. Tronconi, Urea-SCR Technology for deNOx After Treatment of Diesel Exhausts (2014).

[4] M. Colombo, I. Nova, E. Tronconi, A comparative study of the NH3-SCR reactions over a Cu-zeolite and a Fe-zeolite catalyst, Catalysis Today; Diesel emissions control catalysis 151 (2010) 223-230.

[5] A. Scheuer, W. Hauptmann, A. Drochner, J. Gieshoff, H. Vogel, M. Votsmeier, Dual layer automotive ammonia oxidation catalysts: Experiments and computer simulation, Applied Catalysis B: Environmental 111–112 (2012) 445-455.

[6] A. Güthenke, D. Chatterjee, M. Weibel, B. Krutzsch, P. Kočí, M. Marek, I. Nova, E. Tronconi, Current status of modeling lean exhaust gas aftertreatment catalysts, in: Guy B. Marin (Ed.), Advances in Chemical Engineering, Academic Press, 2007, pp. 103-283.

[7] A. Schuler, M. Votsmeier, P. Kiwic, J. Gieshoff, W. Hautpmann, A. Drochner, H. Vogel, NH3-SCR on Fe zeolite catalysts – From model setup to NH3 dosing, Chem. Eng. J. 154 (2009) 333-340.

[8] S. Malmberg, M. Votsmeier, J. Gieshoff, N. Soeger, L. Mussmann, A. Schuler, A. Drochner, Dynamic phenomena of SCR-catalysts containing Fe-exchanged zeolites - experiments and computer simulations, Topics in Catalysis 42-43 (2007) 33-36.

[9] D. Chatterjee, T. Burkhardt, M. Weibel, I. Nova, A. Grossale, E. Tronconi, Numerical Simulation of Zeolite- and V-Based SCR Catalytic Converters, SAE Technical Paper 2007-01-1136 (2007).

[10] D. Chatterjee, P. Koci, V. Schmeisser, M. Marek, M. Weibel, B. Krutzsch, Modelling of a combined storage and -SCR catalytic system for Diesel exhaust gas aftertreatment, Catalysis Today 151 (2010) 395-409.

[11] M. Colombo, I. Nova, E. Tronconi, V. Schmeißer, B. Bandl-Konrad, L. Zimmermann, Experimental and modeling study of a dual-layer (SCR + PGM) NH3 slip monolith catalyst (ASC) for automotive SCR aftertreatment systems. Part 1. Kinetics for the PGM component and analysis of SCR/PGM interactions, Applied Catalysis B: Environmental 142–143 (2013) 861-876.

[12] M. Colombo, I. Nova, E. Tronconi, V. Schmeißer, B. Bandl-Konrad, L.R. Zimmermann, Experimental and modeling study of a dual-layer (SCR + PGM) NH3 slip monolith catalyst (ASC) for automotive SCR after treatment systems. Part 2.

Validation of PGM kinetics and modeling of the dual-layer ASC monolith, Applied Catalysis B: Environmental 142–143 (2013) 337-343.

[13] S. Shrestha, M.P. Harold, K. Kamasamudram, A. Yezerets, Selective oxidation of ammonia on mixed and dual-layer Fe-ZSM-5 + Pt/Al2O3 monolithic catalysts, Catalysis Today 231 (2014) 105-115.

[14] K. Kamasamudram, A. Yezerets, X. Chen, N. Currier, M. Castagnola, H. Chen, New Insights into Reaction Mechanism of Selective Catalytic Ammonia Oxidation Technology for Diesel Aftertreatment Applications, - SAE Int. J. Engines (2011) - 1810.

[15] W. Hauptmann, M. Votsmeier, H. Vogel, D.G. Vlachos, Modeling the simultaneous oxidation of CO and H2 on Pt - Promoting effect of H2 on the CO-light-off, Appl. Catal., A 397 (2011) 174-182.

[16] M. Votsmeier, A. Scheuer, A. Drochner, H. Vogel, J. Gieshoff, Simulation of automotive NH3 oxidation catalysts based on pre-computed rate data from mechanistic surface kinetics, Catalysis Today 151 (2010) 271-277.

[17] S. Samuel, L. Austin, D. Morrey, Automotive test drive cycles for emission measurement and real-world emission levels - a review, Proceedings of the Institution of Mechanical Engineers, Part D: Journal of Automobile Engineering 216 (2002) 555-564.

[18] W. Hauptmann, A. Schuler, J. Gieshoff, M. Votsmeier, Modellbasierte Optimierung der Harnstoffdosierung für SCR-Katalysatoren, Chemie Ingenieur Technik 83 (2011) 1681-1687.

[19] K. Kamasamudram, C. Henry, N. Currier, A. Yezerets, N2O Formation and Mitigation in Diesel Aftertreatment Systems, - SAE Int. J. Engines (2012) - 688.

Chapter 4 - Summary and Conclusions

This work focused on effective catalytic converter design for NO_x removal in diesel vehicles. Models for the SCR and ASC were used, allowing for simulation studies to be completed to make comparisons between different catalytic converters and catalytic converter systems (i.e., a front-end SCR and a back-end ASC) throughout driving cycles.

The first challenge addressed was the need for a method that allows for the simple, automated optimization of an ammonia dosing strategy throughout driving cycles that could be used for catalytic converter screenings. The goal of this strategy was to maximize the NO_x conversion while maintaining the ammonia slip below acceptable regulatory levels. A strategy was presented in Chapter 2 that related the catalyst temperature to a desired surface coverage via entries in a look-up table at each time instant in a driving cycle, and a controller would add the amount of ammonia needed at the succeeding time instant such that the actual surface coverage reaches the desired level.

Using this strategy, the importance of an optimized dosing strategy for each individual catalytic converter system during the design phase was demonstrated. This was completed by making comparisons between an iron zeolite and copper zeolite catalyst as well as different catalyst volumes for the selection of the next-generation catalyst. The optimized dosing strategy was also compared to a simple constant alpha (constant NH_3/NO_x) dosing strategy, which demonstrated that the simple strategy did

not show the extent of the catalytic converter performance difference in screenings compared to when using an optimized dosing strategy. Finally, it was shown that the look-up table dosing strategy is robust owing to the table's dependence on catalyst temperature, which then dictates an ammonia surface coverage level; this means that the optimized entries of the look-up table can be applied to other driving cycles and generally achieve close to the optimized NO_x conversion for the specific driving cycle while generally satisfying the ammonia slip constraints. The robustness is promising in the context of real driving emissions, where an optimized table could be used for randomly generated driving cycles.

The application of the dosing strategy to make comparisons between catalytic converter systems, that is, between an 8" SCR and a 6" SCR + 2" ASC was presented in Chapter 3. The purpose of the work described in this chapter was to investigate the ASC's influence on the catalytic converter performance. In this investigation, it was observed that the ASC can allow for more aggressive ammonia dosing owing to its ability to oxidize the ammonia. This results in a higher NO_x conversion at lower temperatures compared to an SCR-only system, because of the ASC's conversion of ammonia to nitrogen and N_2O; however, NO_x is formed at higher temperatures. Therefore, throughout a transient driving cycle such as the WHTC, no real increase in NO_x conversion is seen between the 8" SCR and the 6" SCR + 2" ASC system. When over-dosing throughout the driving cycle, which could result from catalyst aging or unpredictable driving conditions, it was seen how the ASC acts as a safeguard as it maintains the ammonia slip at a much lower level at little NO_x conversion loss compared to the SCR-only system. In periods of under-dosing, the SCR + ASC

system also allowed for a higher NO_x conversion compared to the 8" SCR, which occurred because more ammonia was still being added to the system than in the 8" SCR. Overall, it was concluded that the ASC is a positive addition to the SCR in meeting the exhaust emission regulations.

4.1 Future Work

Following this investigation, it is important to mention that there are still items to be addressed. First of all, it was assumed that maximum or close-to-maximum NO_x conversions are achieved using the presented optimized dosing strategy in Chapter 2; however, this assumption needs to be verified. To determine how close the presented ammonia dosing strategy is to achieving the maximum NO_x conversion, the optimal dosing profile, or amount of ammonia to be added at each time instant of the driving cycle, needs to be determined. This would result in a large, 1800-parameter optimization problem to be solved (1800 s driving cycle, 1 s time step). Additionally, the SCR model is treated as a black box in the current optimization of the look-up table's entries. Including the SCR model as a system of differential equations for the optimization problem, rather than the black box, could allow for the true optimum to be determined.

The presented dosing strategy should also be validated through implementation at the engine test bench. If the dosing strategy works at the test bench and leads to results similar to the simulation study, future catalytic converter screenings could also take place there. Factors that could lead to varying results from the simulation study include the table's dependence on surface coverage. The simulation study assumed

that the surface coverage is known whereas it has to be estimated at the engine test bench.

Finally, a sensitivity analysis of the ASC design parameters should be completed to understand what configuration would assist in increasing the catalytic converter system performance during the given driving cycle. This would encompass determining the optimal SCR to ASC length for the SCR + ASC configuration, along with the influence of the ASC layer's washcoat loading.

Bibliography

M. Koebel, M. Elsener, M. Kleemann, Urea-SCR: a promising technique to reduce NOx emissions from automotive diesel engines, Catalysis Today 59 (2000) 335-345.

S. Roy, M.S. Hegde, G. Madras, Catalysis for NOx abatement, Appl. Energy 86 (2009) 2283-2297.

D. Peitz, A.M. Bernhard, M. Mehring, M. Elsener, O. Kröcher, Harnstoffhydrolyse für die selektive katalytische Reduktion von NOx: Vergleich der Flüssig- und Gasphasenzersetzung, Chemie Ingenieur Technik 85 (2013) 625-631.

M. Colombo, I. Nova, E. Tronconi, A comparative study of the NH3-SCR reactions over a Cu-zeolite and a Fe-zeolite catalyst, Catalysis Today; Diesel emissions control catalysis 151 (2010) 223-230.

A. Schuler, M. Votsmeier, P. Kiwic, J. Gieshoff, W. Hautpmann, A. Drochner, H. Vogel, NH3-SCR on Fe zeolite catalysts – From model setup to NH3 dosing, Chem. Eng. J. 154 (2009) 333-340.

J.N. Chi, Control Challenges for Optimal NOx Conversion Efficiency from SCR Aftertreatment Systems, - 2009-01-0905 (2009).

F. Willems, R. Cloudt, E. van den Eijnden, M. van Genderen, R. Verbeek, B. de Jager, W. Boomsma, I. van den Heuvel, Is Closed-Loop SCR Control Required to Meet Future Emission Targets?, - 2007-01-1574 (2007).

M. Shost, J. Noetzel, M. Wu, T. Sugiarto, T. Bordewyk, G. Fulks, G.B. Fisher, Monitoring, Feedback and Control of Urea SCR Dosing Systems for NOx Reduction: Utilizing an Embedded Model and Ammonia Sensing, SAE Technical Paper 2008-01-1325 (2008).

A. Güthenke, D. Chatterjee, M. Weibel, B. Krutzsch, P. Kočí, M. Marek, I. Nova, E. Tronconi, Current status of modeling lean exhaust gas aftertreatment catalysts, in: Guy B. Marin (Ed.), Advances in Chemical Engineering, Academic Press, 2007, pp. 103-283.

E.N. Fuller, P.D. Schettler, J.C. Giddings, A new method for prediction of binary gas-phase diffusion coefficients, J. Ind. Eng. Chem. 58 (1966) 18-27.

E. Tronconi, P. Forzatti, Adequacy of lumped parameter models for SCR reactors with monolith structure, AIChE Journal 38 (1992) 201-210.

W. Hauptmann, M. Votsmeier, H. Vogel, D.G. Vlachos, Modeling the simultaneous oxidation of CO and H2 on Pt - Promoting effect of H2 on the CO-light-off, Appl. Catal., A 397 (2011) 174-182.

S. Malmberg, M. Votsmeier, J. Gieshoff, N. Soeger, L. Mussmann, A. Schuler, A. Drochner, Dynamic phenomena of SCR-catalysts containing Fe-exchanged zeolites - experiments and computer simulations, Topics in Catalysis 42-43 (2007) 33-36.

D. Chatterjee, T. Burkhardt, M. Weibel, I. Nova, A. Grossale, E. Tronconi, Numerical Simulation of Zeolite- and V-Based SCR Catalytic Converters, SAE Technical Paper 2007-01-1136 (2007).

D. Chatterjee, P. Koci, V. Schmeisser, M. Marek, M. Weibel, B. Krutzsch, Modelling of a combined storage and -SCR catalytic system for Diesel exhaust gas aftertreatment, Catalysis Today 151 (2010) 395-409.

M. Colombo, I. Nova, E. Tronconi, V. Schmeisser, B. Bandl-Konrad, L. Zimmermann, NO/NO2/N2O-NH3 SCR reactions over a commercial Fe-zeolite catalyst for diesel exhaust aftertreatment: Intrinsic kinetics and monolith converter modelling, Applied Catalysis B: Environmental 111-112 (2012) 106-118.

A. Scheuer, W. Hauptmann, A. Drochner, J. Gieshoff, H. Vogel, M. Votsmeier, Dual layer automotive ammonia oxidation catalysts: Experiments and computer simulation, Applied Catalysis B: Environmental 111–112 (2012) 445-455.

W. Hauptmann, A. Schuler, J. Gieshoff, M. Votsmeier, Modellbasierte Optimierung der Harnstoffdosierung für SCR-Katalysatoren, Chemie Ingenieur Technik 83 (2011) 1681-1687.

S. Samuel, L. Austin, D. Morrey, Automotive test drive cycles for emission measurement and real-world emission levels - a review, Proceedings of the Institution of Mechanical Engineers, Part D: Journal of Automobile Engineering 216 (2002) 555-564.

T.J. Barlow, S. Latham, I.S. McCrae, P.G. Boulter, A reference book of driving cycles for use in the measurement of road vehicle emissions PPR354 (2009).

A.M. Bernhard, D. Peitz, M. Elsener, T. Schildhauer, O. Kroecher, Catalytic urea hydrolysis in the selective catalytic reduction of NOx: catalyst screening and kinetics on anatase TiO2 and ZrO2., Catalysis Science & Technology 3 (2013) 942-951.

M. Weiss, P. Bonnel, R. Hummel, N. Steininger, A complementary emissions test for light-duty vehicles: Assessing the technical feasibility of candidate procedures EUR 25572 EN (2013).

M. Weibel, V. Schmeißer, F. Hofmann, Model-Based Approaches to Exhaust Aftertreatment System Development, in: I. Nova, E. Tronconi (Eds.), Springer New York, 2014, pp. 691-707.

I. Nova, E. Tronconi, Urea-SCR Technology for deNOx After Treatment of Diesel Exhausts (2014).

A. Scheuer, W. Hauptmann, A. Drochner, J. Gieshoff, H. Vogel, M. Votsmeier, Dual layer automotive ammonia oxidation catalysts: Experiments and computer simulation, Applied Catalysis B: Environmental 111–112 (2012) 445-455.

M. Colombo, I. Nova, E. Tronconi, V. Schmeißer, B. Bandl-Konrad, L. Zimmermann, Experimental and modeling study of a dual-layer (SCR + PGM) NH3 slip monolith catalyst (ASC) for automotive SCR aftertreatment systems. Part 1. Kinetics for the PGM component and analysis of SCR/PGM interactions, Applied Catalysis B: Environmental 142–143 (2013) 861-876.

M. Colombo, I. Nova, E. Tronconi, V. Schmeißer, B. Bandl-Konrad, L.R. Zimmermann, Experimental and modeling study of a dual-layer (SCR + PGM) NH3

slip monolith catalyst (ASC) for automotive SCR after treatment systems. Part 2. Validation of PGM kinetics and modeling of the dual-layer ASC monolith, Applied Catalysis B: Environmental 142–143 (2013) 337-343.

S. Shrestha, M.P. Harold, K. Kamasamudram, A. Yezerets, Selective oxidation of ammonia on mixed and dual-layer Fe-ZSM-5 + Pt/Al2O3 monolithic catalysts, Catalysis Today 231 (2014) 105-115.

K. Kamasamudram, A. Yezerets, X. Chen, N. Currier, M. Castagnola, H. Chen, New Insights into Reaction Mechanism of Selective Catalytic Ammonia Oxidation Technology for Diesel Aftertreatment Applications, - SAE Int. J. Engines (2011) - 1810.

M. Votsmeier, A. Scheuer, A. Drochner, H. Vogel, J. Gieshoff, Simulation of automotive NH3 oxidation catalysts based on pre-computed rate data from mechanistic surface kinetics, Catalysis Today 151 (2010) 271-277.

K. Kamasamudram, C. Henry, N. Currier, A. Yezerets, N2O Formation and Mitigation in Diesel Aftertreatment Systems, - SAE Int. J. Engines (2012) - 688.